Spring 2018 – Systems Biology of Reproduction
Discussion Outline – Hypothalamus-Pituitary Development & Function
Michael K. Skinner – Biol 475/575
CUE 418, 10:35-11:50 am, Tuesday & Thursday
March 29, 2018
Week 12

Hypothalamus-Pituitary Development & Function

Primary Papers:

1. Belchetz et al. (1978) Science 202:631
2. Houlahan et al. (2015) Toxicology 328:93-101
3. Kuhnen et al. (2016) Cell Metabolism 24:502-509

Discussion

Student 4: Reference 1 above

- What unique endocrine parameter was identified in the hypothalamic regulation of pituitary function?
- What physiological advantage does this have?
- How does this information fit into the understanding of Brain-Pituitary-Gonadal axis?

Student 5: Reference 2 above

- What was the experimental design and objectives of the study?
- What cellular processes and pathways were identified to be effected?
- What insights into dioxin actions on the hypothalamus were obtained?

Student 6: Reference 3 above

- What was the experimental design and objective of study?
- What alteration in the POMC was identified and how?
- What mechanism is suggested for the etiology of obesity?

scouring is less pronounced because of the lack of fracturing; (iii) the narrowness of the river allows more of the debris to be swept away; and (iv) the limestone, although resistant, appears to shed less large-size debris.

With the evidence of a consistent structural influence, we offer this generalized model for the rapid-pool-tributary sequences along the Colorado. Large faults determine zones of bedrock weakness within the Grand Canyon. Structures that run perpendicular to the river provide an advantage for side canyon drainage. The side canyon tributaries, flowing within the brecciated zones, deliver material to the main river that is too large to be carried downstream. This material forms a channel constriction, accelerated flow, and a rapid. Part of the accelerated flow at the foot of the rapids is directed downward against the bed. These high velocities, coupled with the zone of brecciation associated with the faulted bedrock, lead to deep scour below the rapids, and thus the deep pools. The hydraulic processes (autogenic) that produce regularly spaced riffles (5) on most streams, therefore, may dominate a few sections of the Colorado River in the Grand Canyon, but along most of its course these processes appear to be superimposed on, or modified by, local external (exogenic) controls.

ROBERT DOLAN
ALAN HOWARD
Department of Environmental Sciences, University of Virginia, Charlottesville 22903

DAVID TRIMBLE
North American Exploration, Berkmar Drive, Charlottesville, Virginia 22901

References and Notes

1. L. Leopold, *U.S. Geol. Surv. Prof. Pap. 669* (1969), pp. 131–145.
2. R. Dolan, A. Howard, A. Gallenson, *Am. Sci.* 62, 492 (1974).
3. W. K. Hamblin and J. K. Rigby, *Guidebook to the Colorado River*, part 1, *Lee's Ferry to Phantom Ranch in Grand Canyon National Park* (Brigham Young Univ. Press, Provo, Utah, 1968); *Guidebook to the Colorado River*, part 2, *Phantom Ranch in Grand Canyon National Park* (Brigham Young Univ. Press, Provo, Utah, 1969).
4. P. W. Huntoon, in *Geology of the Grand Canyon*, W. J. Breed and E. C. Root, Eds. (Museum of Northern Arizona, Flagstaff, 1974), pp. 82–115.
5. E. A. Keller and W. N. Melhorn, *Geol. Soc. Am. Bull.* 89, 723 (1978).

27 February 1978; revised 24 May 1978

Hypophysial Responses to Continuous and Intermittent Delivery of Hypothalamic Gonadotropin-Releasing Hormone

Abstract. *In rhesus monkeys with hypothalamic lesions that abolish gonadotropic hormone release by the pituitary gland, the constant infusion of exogenous gonadotropin-releasing hormone (GnRH) fails to restore sustained gonadotropin secretion. In marked contrast, intermittent administration of the synthetic decapeptide once per hour, the physiological frequency of gonadotropin release in the monkey, reestablishes pituitary gonadotropin secretion. This phenomenon is attributable to the pattern of GnRH delivery rather than to the amounts of this hormone to which the cells of the pituitary are exposed. Moreover, the initiation of continuous GnRH administration in animals with lesions and in which gonadotropin secretion is reestablished by intermittent GnRH replacement can result in a "desensitization" or "down regulation" of the processes responsible for gonadotropin release.*

Lesions induced by radio-frequency current in the medial basal hypothalamus of rhesus monkeys (*1*) abolish the secretion of the gonadotropic hormones [luteinizing hormone (LH) and follicle-stimulating hormone (FSH)] by the pituitary gland, presumably by interfering with the release of the hypothalamic gonadotropin-releasing hormone, GnRH. Attempts to restore gonadotropin secretion in such animals by the continuous infusion of synthetic GnRH succeeded only in eliciting an evanescent release of LH and FSH despite the continued administration of the decapeptide (*1*). When, on the other hand, GnRH was administered once per hour (*2*), a rate equivalent to the physiological frequency of episodic LH release in ovariectomized monkeys (*3*), sustained increases in plasma LH and FSH concentrations were achieved for the duration of the replacement regimen (up to 7 weeks). The study described here was designed to determine whether the refractoriness of the pituitary to the continuous infusion of GnRH is attributable to the pattern of hypophysiotropic hormone stimulation per se or to the quantity of the decapeptide delivered to the pituitary.

Cardiac catheters were implanted in seven ovariectomized rhesus monkeys (4.2 to 6.8 kg of body weight) in which gonadotropin secretion had been abolished or severely curtailed by placement of radio-frequency lesions in the hypothalamus (*1*). By means of an infusion-withdrawal device that permits continuous access to the venous circulation without the animal being restrained, GnRH (*4*) was infused continuously by way of the cardiac catheter at rates of 0.001, 0.01, 0.1, and 1.0 μg per minute as described (*2*). Each infusion rate was maintained for 10 days (*5*). Blood samples were taken daily by way of the catheter, or by femoral venipuncture after the animal was sedated (30 to 40 mg of sodium thiamylal per animal, intravenously), and plasma concentrations of LH and FSH were determined by use of established radioimmunoassays (*6*). The pituitary response to GnRH administered at the rate of 1 μg per minute for 6 minutes once per hour was determined in similar fashion.

The mean circulating LH and FSH concentrations during the last 5 days of each continuous GnRH infusion, which reflected the steady-state response of the pituitary to this mode of hypophysiotropic stimulation (*7*), are shown in Fig. 1A. None of the continuous infusions of releasing hormone produced a sustained increment in plasma LH and FSH concentrations. In sharp contrast, however, long-term restoration of gonadotropin secretion was achieved in the same animals by the intermittent administration of GnRH (Fig. 1B). These observations lead to the conclusion that the failure of continuous GnRH infusion, regardless of infusion rate, to initiate sustained gonadotropin secretion in ovariectomized monkeys bearing hypothalamic lesions is the consequence of the pattern of GnRH administration rather than of the total mass of the decapeptide delivered to the gonadotrophs.

The effects on gonadotropin secretion of a shift in GnRH administration from the intermittent to the continuous mode, without a change in the infusion rate, were investigated in four similarly prepared monkeys in which gonadotropin secretion had been reestablished by pulsatile hypophysiotropic stimulation. The institution of continuous GnRH administration was followed by a brief increase in plasma LH and FSH lasting approximately 5 hours. Thereafter, however, circulating gonadotropin declined, reaching a nadir within 7 to 10 days where they remained for the duration of the continuous infusion period. This inhibition was reversed when pulsatile GnRH administration was reinstituted (Fig. 2).

These influences of pattern of hypophysiotropic stimulation may be related to the phenomenon of "desensitization" or "down regulation" (*8*), whereby pro-

0036-8075/78/1110-0631$00.50/0

longed exposure to a high circulating concentration of hormone or drug results in a decrease in the response of the target tissue. Continuous infusions of GnRH, albeit of relatively short duration, have also been reported to result in the development of pituitary refractoriness in rats and sheep (*9*). The phenomenon of "down regulation," which has been described for insulin, LH, and catecholamines, may result, in part, from a reduction in available receptors for the agonist (*10*). A decline in the number of growth hormone receptors on lymphocytes, and of thyrotropin-releasing factor receptors on a clonal strain of pituitary cells has also been reported after long-term exposure to the homologous hormone (*11*). In relating the association between receptor loss and "down regulation" to the present findings, it is tempting to speculate that an intermittent supply of GnRH permits the regeneration of its receptors, whereas the continuous mode of hypophysiotropic stimulation does not. Whatever the underlying cellular mechanism responsible for our findings may be, it appears that the intermittent mode of GnRH stimulation is optimal in eliciting gonadotropin secretion, thereby underlining the physiologic significance of the pulsatile nature of endogenous GnRH release by the hypothalamus (*3*, *12*).

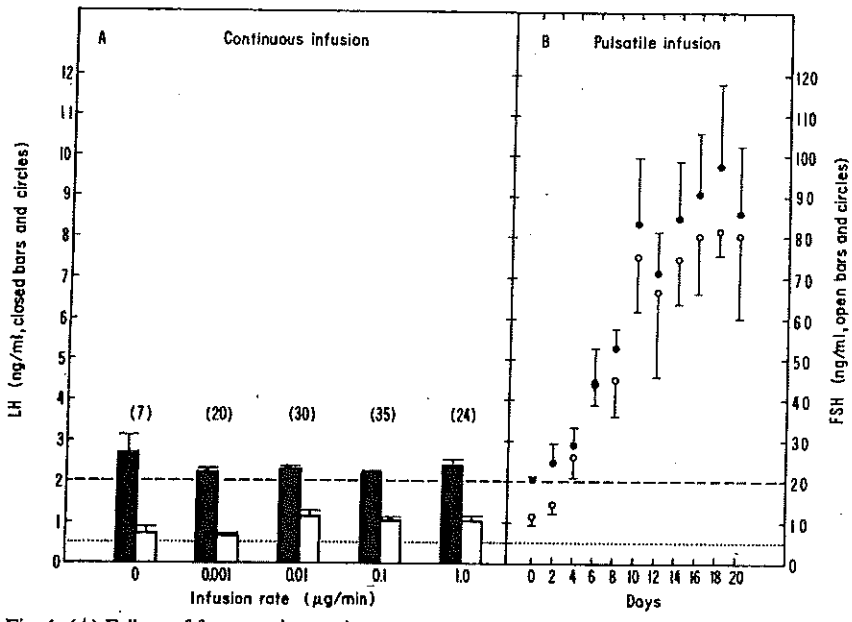

Fig. 1. (A) Failure of four continuous intravenous GnRH infusion rates to reestablish gonadotropin secretion in ovariectomized rhesus monkeys bearing hypothalamic lesions. Each bar represents the mean ± standard error (S.E.) of the number of observations in parentheses obtained during the last 5 days of the infusion period. Plasma gonadotropin concentrations during the control period were obtained just before the initiation of the GnRH infusions. (B) Effect of an intermittent GnRH infusion (1 μg/min for 6 minutes once per hour) on gonadotropin secretion in the same animals shown in (A). Each point is the mean ± S.E. of three to five observations. The horizontal dots and dashes show the sensitivity limits of the FSH and LH assays, respectively.

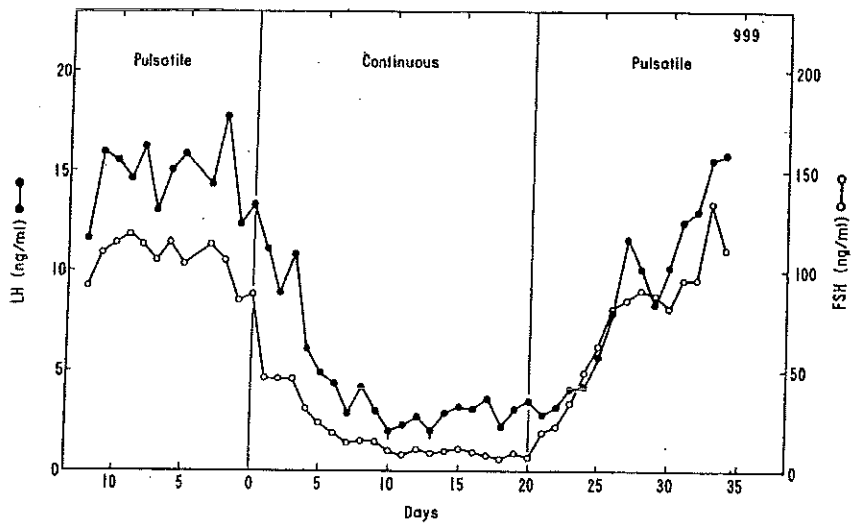

Fig. 2. Suppression of plasma LH and FSH concentrations after initiation, on day 0, of a continuous GnRH infusion (1 μg/min) in an ovariectomized rhesus monkey with a radio-frequency lesion in the hypothalamus; gonadotropin secretion had been reestablished by the intermittent (pulsatile) administration of the decapeptide (1 μg/min for 6 minutes once per hour). The inhibition of gonadotropin secretion was reversed after reinstitution of the intermittent mode of GnRH stimulation on day 20. The vertical lines beneath the LH data points on days 10 and 13 of the continuous infusion regimen indicate values below the sensitivity of the radioimmunoassay.

P. E. Belchetz*
T. M. Plant, Y. Nakai†
E. J. Keogh‡, E. Knobil
Department of Physiology, University of Pittsburgh School of Medicine, Pittsburgh, Pennsylvania 15261

References and Notes

1. T. M. Plant, L. C. Krey, J. Moossy, J. T. McCormack, D. L. Hess, E. Knobil, *Endocrinology* **102**, 52 (1978).
2. Y. Nakai, T. M. Plant, D. L. Hess, E. J. Keogh, E. Knobil, *ibid.*, p. 1008.
3. D. J. Dierschke, A. N. Bhattacharya, L. E. Atkinson, E. Knobil, *ibid.* **87**, 850 (1970).
4. Stock solutions of synthetic GnRH, provided by R. Guillemin (LRF, 14-200-500 and 14-136-06), Abbott Laboratories (lot-34-414AL), and the National Institutes of Health (lot 26-306AL), were prepared in 0.01*M* acetic acid in 0.9 percent NaCl and stored in small portions at −85°C. Prior to use, portions were thawed and diluted with sterile saline for infusion.
5. The GnRH was infused in both ascending (four animals) and descending (three animals) rate sequences with the same results.
6. F. J. Karsch, R. F. Weick, W. R. Butler, D. J. Dierschke, L. C. Krey, G. Weiss, J. Hotchkiss, T. Yamaji, E. Knobil, *Endocrinology* **92**, 1740 (1973); T. Yamaji, W. D. Peckham, L. E. Atkinson, D. J. Dierschke, E. Knobil, *ibid.*, p. 1652. The heterologous FSH assay has been modified in the following manner. A new FSH preparation from the rhesus monkey, *Macaca mulata* (WP-XIII-21-42) is now used as the standard. The immunopotency of this preparation is 1.2 times that of the original standard (WDP-XI-93-4546). A new human FSH antiserum (batch 4, NIAMDD-NPA) is employed. This has increased the sensitivity of the assay to 5 ng of WP-XIII-21-42 per milliliter. The sensitivity of the LH radioimmunoassay is 2 ng of the standard (WDP-X-47-BC) per milliliter.
7. The transient discharge of gonadotropin described previously during the initiation of continuous GnRH administration (*1*) was also observed in this study at the highest GnRH infusion rate (1 μg/min). This sudden release of gonadotropin, which resulted in a marked increase in circulating LH and FSH concentrations 7 to 10 hours after initiation of continuous infusion followed by a decline to control levels within 2 days was only observed, however, in the three animals which received the highest GnRH infusion rate first.
8. K. J. Catt and M. L. Dufau, *Annu. Rev. Physiol.* **39**, 529 (1977).
9. P. K. Chakraborty, T. E. Adams, G. K. Tarnavsky, J. J. Reeves, *J. Anim. Sci.* **39**, 1150 (1974); E. L. Piper, J. L. Perkins, D. R. Tugwell, W. G. Vaught, *Proc. Soc. Exp. Biol. Med.* **148**, 880 (1975); G. A. Schuiling, J. De Koning, A. F. Zurcher, H. P. Gnodde, G. P. van Rees, *Neuroendocrinology* **20**, 151 (1976).
10. J. R. Gavin, J. Roth, D. M. Neville, P. deMeyts, D. N. Buell, *Proc. Natl. Acad. Sci. U.S.A.* **71**, 84 (1974); C. Mukherjee, M. C. Caron, R. J. Lef-

kowitz, *ibid.* 72, 1945 (1975); A. J. W. Hsueh, M. L. Dufau, K. J. Catt, *ibid.* 74, 592 (1977); A. H. Soll, C. R. Kahn, D. M. Neville, J. Roth, *J. Clin. Invest.* 56, 769 (1975); J. Roth *et al.*, *Recent Prog. Horm. Res.* 31, 95 (1975); A. J. W. Hsueh, M. L. Dufau, K. J. Catt, *Biochem. Biophys. Res. Commun.* 72, 1145 (1976); R. J. Ryan, L. Birnbaumer, C. Y. Lee, M. Hunzicker-Dunn, *Int. Rev. Physiol.* 13, 85 (1977); M. Conti, J. P. Harwood, M. L. Dufau, K. J. Catt, *Mol. Pharmacol.* 13, 1024 (1977).

11. P. M. Hinkle and A. H. Tashjian, *Biochemistry* 14, 3845 (1975); M. A. Lesniak and J. Roth, *J. Biol. Chem.* 251, 3720 (1976).
12. P. W. Carmel, S. Araki, M. Ferin, *Endocrinology* 99, 243 (1976); V. L. Gay and N. A. Sheth, *ibid.* 90, 158 (1972); W. R. Butler, P. V. Malvern, L. B. Willett, D. J. Bolt, *ibid.* 91, 793 (1972); C. B. Katongole, F. Naftolin, R. V. Short, *J. Endocrinol.* 50, 457 (1971); H. R. Nankin and P. Troen, *J. Clin. Endocrinol. Metab.* 33, 558 (1971); S. S. C. Yen *et al.*, *ibid.* 34, 671 (1972).

13. Supported by NIH grants HD03968 and HD08610, by a grant from the Ford Foundation, by a Peel Medical Trust postdoctoral research fellowship and Fulbright-Hays travel grant to P.E.B., by an NIH postdoctoral fellowship to T.M.P., and by a PHS international fellowship to E.J.K. We thank Dr. Roger Guillemin, the National Institutes of Health, and Abbott Laboratories for the synthetic GnRH and R. L. Shields, J. Gunnett, C. Stehle, M. Kruth, M. Forston, and our animal care staff for expert technical assistance.

* Present address: Endocrine Unit, St. Bartholomew's Hospital, West Smithfield, London EC1, England.
† Present address: Department of Medicine, Kyoto University, 53, Shogoin Kawahara-Cho, Sakyo-Ku, Kyoto, Japan.
‡ Present address: Endocrinology Unit, Sir Charles Gairdner Hospital, Queen Elizabeth II Medical Centre, Nedlands, Western Australia, 6009.

10 April 1978; revised 14 June 1978

Slow Axonal Transport of Neurofilament Proteins: Impairment by β,β'-Iminodipropionitrile Administration

Abstract. *β,β'-Iminodipropionitrile (IDPN) administration prevented normal slow axonal transport of [^{35}S]methionine- or [^{3}H]leucine-labeled proteins in rat sciatic motor axons. Ultrastructural and electrophoretic studies showed that the neurofilament triplet proteins in particular were retained within the initial 5 millimeters of the axons, resulting in neurofilament-filled axonal swellings. Fast anterograde and retrograde axonal transport were not affected. The IDPN thus selectively impaired slow axonal transport. The neurofibrillary pathology in this model is the result of the defective slow transport of neurofilaments.*

The axon utilizes special systems of cytoplasmic motility to convey materials along its length. These axonal transport systems are generally distinguished, on the basis of direction and rate of movement, into fast, slow, and intermediate anterograde transport (conveying materials away from the cell body) and retrograde transport (carrying materials toward the cell body) (*1*). Neither the mechanisms of transport nor the relationships between these systems are fully defined. A unitary mechanism for all types of transport has been proposed in which the differences in rate are related to the proportion of time that various transported materials are associated with the transport mechanism (*2*). Alternatively, a mechanism for slow transport distinct from that for bidirectional rapid transport has been suggested (*3*).

Identification of selective effects of pharmacologic agents on the various transport systems provides one approach to further studies of the mechanisms and the interrelationships of the axonal transport systems. In this study, we have examined the effects on axonal transport of β,β'-iminodipropionitrile (IDPN). Previous studies (*4*, *5*) have shown that IDPN administration produces large neurofilament-filled swellings in the most proximal portion of the axon. Since neurofilaments are known to be carried by slow transport (*1*, *3*), this pathology suggested that IDPN might have an effect on slow transport. Our results show that IDPN selectively impairs slow axonal transport, without direct effects on fast or retrograde transport. This model is of special interest, since it represents the first disorder in which the pathogenesis of neurofibrillary pathology can be reconstructed.

Slow axonal transport was studied by injecting [^{3}H]leucine or [^{35}S]methionine into the lumbar ventral horns of Sprague-Dawley or Wistar rats (*6*). The animals were returned to their cages, and 1 to 8 weeks later they were killed. The sciatic nerves were rapidly removed and divided into 5-mm segments. These nerve segments were each homogenized manually in a mixture of sodium dodecyl sulfate, urea, and β-mercaptoethanol (*3*) and heated to 100°C for 4 minutes. After centrifugation, only a minute residuum remained undissolved, and essentially all the radioactivity in the segments was solubilized (*3*). To construct curves of the distribution of radioactivity along the nerve, an aliquot of each sample was counted by liquid scintillation techniques, and counts per minute for each segment were plotted against the position of the segment along the nerve (*3*, *6*).

In addition, to determine the pattern of migration of individual slowly transported proteins, portions of the samples were subjected to electrophoresis on polyacrylamide slab gels (*7*); the gels were then impregnated with 2,5-phenyloxazole and dried, and fluorograms were prepared by exposure of Kodak type RP x-ray film to the gels for 2 weeks to 4 months (*7*). [The x-ray film was preexposed to a measured light flash (*8*).] The resulting fluorograms revealed the relative amounts of individual labeled proteins in each segment of nerve.

The IDPN (Eastman Kodak, Rochester, N.Y.) was administered in one of two ways: by intraperitoneal injection of 1 or 2 g/kg, or by sustained exposure to 0.05 percent IDPN in the drinking water only (*9*). Because of the different means of administration, transport studies were performed on animals ranging from 3 to 12 months of age. Age-matched controls, purchased at the same time as experimental animals, were used in all studies.

In 14 normal animals the curves of slow transport were similar to those previously reported (*1*, *3*), with the major slow component peak moving down the nerve at 1.5 to 2 mm/day (in 200-g animals) (Fig. 1a). The fluorograms from these control animals (Fig. 2a) showed the three major groups of labeled proteins described by Hoffman and Lasek (*3*): actin (molecular weight, 46,000); proteins presumptively identified as tubulin (molecular weights, 53,000 and 57,000); and the neurofilament triplet proteins with estimated molecular weights of 68,000, 145,000, and 200,000 (*3*, *10*). In each of 11 normal rats, the rate of actin and tubulin migration ranged from 0.5 to 5 mm/day, with the density of label greatest in segments corresponding to rates of 1.0 to 3.5 mm/day (Fig. 2a). The neurofilament triplet proteins moved together at a more restricted range of rates of 1 to 2.5 mm/day, coinciding with the major slow component peak (Fig. 2a).

Similar studies were performed with rats injected with IDPN. In these studies IDPN was given either 1 to 2 days before or 1 to 2 days after microinjection of the labeled precursor into the spinal cord. Groups of animals were then killed 7, 14, or 21 days after labeling. At all times after labeling, the major slow transport peak failed to migrate beyond the initial 5 to 10 mm of the ventral roots (Fig. 1b). Gel fluorography (21 days after labeling) showed that movement of all the major slow component proteins was abnormal, with the neurofilament triplet proteins being the most strikingly affected (Fig. 2b). Most of the labeled neurofilament triplet proteins were retained in the initial 5 to 10 mm of the roots; only a small proportion were transported beyond this level. Following injection of IDPN, tubu-

0036-8075/78/1110-0633$00.50/0

Toxicology 328 (2015) 93–101

Contents lists available at ScienceDirect

Toxicology

journal homepage: www.elsevier.com/locate/toxicol

Transcriptional profiling of rat hypothalamus response to 2,3,7,8-tetrachlorodibenzo-ρ-dioxin

Kathleen E. Houlahan [a], Stephenie D. Prokopec [a], Ivy D. Moffat [b], Jere Lindén [c], Sanna Lensu [d,e], Allan B. Okey [b], Raimo Pohjanvirta [f,1], Paul C. Boutros [a,b,g,*]

[a] Informatics and Bio-computing Program, Ontario Institute for Cancer Research, Toronto, Canada
[b] Department of Pharmacology & Toxicology, University of Toronto, Toronto, Canada
[c] The Finnish Food Safety Authority, Helsinki, Finland
[d] Department of Biology of Physical Activity, University of Jyväskylä, Jyväskylä, Finland
[e] Department of Environmental Health, National Institute for Health and Welfare, Kuopio, Finland
[f] Department of Food Hygiene and Environmental Health, University of Helsinki, Helsinki, Finland
[g] Department of Medical Biophysics, University of Toronto, Toronto, Canada

ARTICLE INFO

Article history:
Received 25 November 2013
Received in revised form 12 December 2014
Accepted 16 December 2014
Available online 18 December 2014

Keywords:
AHR
TCDD
Microarray
Hypothalamus
Feed restriction

ABSTRACT

In some mammals, halogenated aromatic hydrocarbon (HAH) exposure causes wasting syndrome, defined as significant weight loss associated with lethal outcomes. The most potent HAH in causing wasting is 2,3,7,8-tetrachlorodibenzo-ρ-dioxin (TCDD), which exerts its toxic effects through the aryl hydrocarbon receptor (AHR). Since TCDD toxicity is thought to predominantly arise from dysregulation of AHR-transcribed genes, it was hypothesized that wasting syndrome is a result of to TCDD-induced dysregulation of genes involved in regulation of food-intake. As the hypothalamus is the central nervous systems' regulatory center for food-intake and energy balance. Therefore, mRNA abundances in hypothalamic tissue from two rat strains with widely differing sensitivities to TCDD-induced wasting syndrome: TCDD-sensitive Long–Evans rats and TCDD-resistant Han/Wistar rats, 23 h after exposure to TCDD (100 μg/kg) or corn oil vehicle. TCDD exposure caused minimal transcriptional dysregulation in the hypothalamus, with only 6 genes significantly altered in Long–Evans rats and 15 genes in Han/Wistar rats. Two of the most dysregulated genes were *Cyp1a1* and *Nqo1*, which are induced by TCDD across a wide range of tissues and are considered sensitive markers of TCDD exposure. The minimal response of the hypothalamic transcriptome to a lethal dose of TCDD at an early time-point suggests that the hypothalamus is not the predominant site of initial events leading to hypophagia and associated wasting. TCDD may affect feeding behaviour via events upstream or downstream of the hypothalamus, and further work is required to evaluate this at the level of individual hypothalamic nuclei and subregions.

1. Introduction

Halogenated aromatic hydrocarbons (HAHs) are a class of toxic compounds widely present within the environment as a result of plastics incineration, electronics recycling, pesticide application and paper bleaching (Linden et al., 2010; Okey 2007). 2,3,7,8-tetrachlorodibenzo-ρ-dioxin (TCDD) is the best-studied HAH, and exposure to it has been linked to teratogenesis, immunosuppression, acute lethality and many other toxicities (Mimura and Fujii-Kuriyama 2003; Pohjanvirta and Tuomisto 1994). Perhaps most significantly in many mammalian models, TCDD causes wasting syndrome–a potentially fatal dose-dependent reduction in body-weight (Linden et al., 2014; Seefeld et al., 1984). Many laboratory animals exposed to TCDD experience hypophagia and appear to defend a lowered body weight set point (Linden et al., 2010; Seefeld et al., 1984). The role of wasting in TCDD-induced lethality remains obscure: dietary interventions such as force feeding and high-energy diets reduce or prevent weight loss, but have minimal impact on mortality (Seefeld et al., 1984; Tuomisto et al., 1999).

* Corresponding author at: 661 University Avenue Toronto, Ontario M5G 0A3, Canada. Tel.:+ 416 673 8564; fax: 416 673 8564.
E-mail addresses: raimo.pohjanvirta@helsinki.fi (R. Pohjanvirta), Paul.Boutros@oicr.on.ca (P.C. Boutros).
[1] Department of Food Hygiene and Environmental Health, Faculty of Veterinary Medicine, P.O. Box 66, FI-00014 University of Helsinki, Helsinki, Finland. Tel.: +358 9 19157147; fax: +358 9 19 157 170.

http://dx.doi.org/10.1016/j.tox.2014.12.016

TCDD toxicity is mediated by the aryl hydrocarbon receptor (AHR), a ligand-responsive transcription factor involved in regulation of cytochrome P450 proteins involved in the phase I xenobiotic metabolism pathway (Mimura and Fujii-Kuriyama 2003; Okey 2007). The AHR is a member of the PAS/basic helix-loop-helix (bHLH) superfamily, with a bHLH domain and two PAS domains within its N-terminus (Dolwick et al., 1993) and a transactivation domain at its C-terminus (Ko et al., 1997). In the absence of ligand, the AHR is cytoplasmic, where it forms a complex with stabilizing chaperone proteins hsp90, ARA9/XAP2 and p23 (Petrulis and Perdew 2002). Activation occurs following ligand binding to the PAS-B domain, which promotes translocation to the nucleus. The AHR then dimerizes with the AHR nuclear translocator (ARNT) (Reyes et al., 1992), and this dimer binds to DNA and regulates transcription. Many lines of evidence indicate that major toxicities from TCDD are caused by dysregulation of AHR target genes (reviewed in Okey 2007).

The hypothalamus is central to regulation of food intake and energy balance, mainly through small peptide signalling molecules. The hypothalamic arcuate nucleus (ARC) translates adipose level signals from peptides (insulin and leptin) to the rest of the CNS by releasing neuropeptides and hormones (Konner et al., 2009). Depending on the stimulus, these peptides may be orexigenic (*e.g.* agouti-related peptide (AgRP) and neuropeptide Y (NPY)) or anorexigenic (*e.g.* α-melanocortin-stimulating hormone (α-MSH) and cocaine-and-amphetamine regulated transcript (CART)). Lesions in hypothalamic nuclei that prevent normal responses to signalling peptides can cause either hypophagia or hyperphagia depending on lesion location (Elmquist et al., 1999; Wang et al., 2013). As such, many groups have hypothesized that TCDD-mediated changes in the hypothalamus underlie the observed wasting syndrome. A previous study discovered a non-additive interaction between ventromedial hypothalamic lesions and TCDD on body weight, suggestive of the involvement of a hypothalamic feed-intake regulation pathway in the wasting syndrome (Tuomisto et al., 1995). TCDD has been previously shown to modulate mRNA abundances of numerous neuropeptides and receptors, particularly orexigenic peptides, in both directions (Linden et al., 2005). Additionally, several components of the AHR-signalling pathway are expressed in the hypothalamus, with three AHR-regulated genes (*Ahrr, Cyp1a1* and *Cyp1a2*) significantly up-regulated in response to TCDD (Korkalainen et al., 2005).

To evaluate the role of TCDD-induced transcriptomic changes in the hypothalamus on observed toxicities, two rat strains that markedly differ in susceptibility to TCDD-induced toxicities were evaluated: TCDD-sensitive Long–Evans (Turku/AB) rats (L–E; LD_{50} ~20 μg/kg for male rats) and TCDD-resistant Han/Wistar (Kuopio) rats (H/W; LD_{50} > 9600 μg/kg) (Pohjanvirta et al., 1995; Unkila et al., 1994). The great resistance of H/W rats to toxicity is due to a point mutation in the intron/exon boundary that causes alternative splicing (Moffat et al., 2007; Pohjanvirta et al., 1998). This leads to variation within the transactivation domain of AHR and alters some responses to TCDD such as resisting lethality (Moffat et al., 2007; Pohjanvirta et al., 1998). Wasting syndrome is another example of this altered response; a mitigated variety of wasting manifests in H/W rats but only after >100-fold higher doses of TCDD than is required in L–E rats (Linden et al., 2010; Pohjanvirta et al., 1998). The use of H/W rats allows for identification of transcriptomic responses that differ from those in susceptible strains (Boutros et al., 2011; Franc et al., 2008). Such differences may identify the key genes whose dysregulation underlies pathogenesis from TCDD exposure.

2. Methods

2.1. Samples

Sixteen male rats, eight L–E and eight H/W, were examined. Rats were housed singly in stainless-steel wire-mesh cages and subjected to light and dark cycles lasting 12 h each, with lights on from 07:00 to 19:00. Animals were fed pelleted R36 feed (Lactamin, Södertälje, Sweden) and provided with tap water. The temperature within the housing environment was 21 ± 1 °C with relative humidity at 50% ± 10%. H/W rats were 15–16 weeks of age upon treatment while L–E rats were 16–22 weeks of age (to compensate for the more rapid growth of H/W rats).

2.2. Animal handling

Four rats from each strain were treated with 100 μg/kg of TCDD dissolved in corn oil vehicle while the remaining four were treated only with corn oil which served as the vehicle control. Animals were distributed such that each group was similarly body weight matched prior to treatment. Treatments were administered by oral gavage. Towards the end of the daily dark phase (between 5:40 and 6:45 a.m.), 23 h post exposure, all rats were euthanized by decapitation. Hypothalamus (incision sites: rostral border of the optic chiasm, caudal border of the mamillary body, ventral border of the anterior commissure and lateral borders of the tuber cinereum and mamillary body complexes) was rapidly removed and snap-frozen in liquid nitrogen. Tissues were stored at −80 °C or lower until processed. All study plans were approved by the Animal Experiment Committee of the University of Kuopio and the Provincial Government of Eastern Finland. All animal handling and reporting comply with ARRIVE guidelines (Kilkenny et al., 2010).

2.3. Sample processing and microarray hybridization

Total mRNA was extracted using Qiagen RNeasy Lipid Tissue Mini kits according to manufacturer's instruction (Qiagen, Mississauga, Canada). Total RNA yield was quantified by UV spectrophotometry and RNA integrity was verified using an Agilent 2100 Bioanalyzer (Agilent Technologies, Santa Clara, CA). RNA from individual rats was hybridized to Affymetrix RAE230-2 arrays at The Centre for Applied Genomics (Toronto, Canada) and RNA abundances were quantified using an Affymetrix GeneChip Scanner 3000.

2.4. Data preparation

Raw microarray data were loaded into the *R* statistical environment (v3.1.0) using the affy package (v1.42.2) of the BioConductor library and the EntrezGene ID map rat2302rnentrezgcdf (v18.0.0) (Dai et al., 2005; Gautier et al., 2004). Raw data were pre-processed using the RMA algorithm (Irizarry et al., 2003) and quality-control plots were generated using the affy (v1.42.2), lattice (v0.20-29) and latticeExtra (v0.6-26) packages to assess sample homogeneity (Supplementary Fig. S1). Unsupervised pattern recognition used the DIANA agglomerative hierarchical clustering algorithm, as implemented in the cluster package (v1.15.2) and Pearson's correlation was used as a similarity metric. The distribution of the coefficient of variations for each gene was analyzed to ensure low inter-replicate variance. All raw and pre-processed microarray data are available in the GEO repository (accession: GSE61039).

Supplementry material related to this article found, in the online version, at http://dx.doi.org/10.1016/j.tox.2014.12.016.

2.5. Statistical analysis

A linear model was fit to each gene using contrasts to relate TCDD treatment and vehicle controls for each rat strain (*i.e.* HWT–HWC and LET–LEC). The variance amongst probes was reduced using an empirical Bayes method (Smyth 2004). Moderated *t*-tests compared each coefficient to zero, while F-tests were applied gene-wise to test for significant differences in variation between the two rat strains. All *p*-values were false discovery-rate adjusted for multiple testing to generate *q*-values (Storey and Tibshirani 2003). Linear modeling and hypothesis testing were completed using the limma package (v3.20.4). Genes were analyzed at multiple *q*-value thresholds to ensure results were threshold-independent, but for primary analyses a threshold $q < 0.05$ was used.

2.6. Data visualization

Inter-strain *p*-value variability was quantified and plotted as above. Inter-strain *p*-value variability plots compared the *p*-value distribution between the two strains when mRNA abundance was both up- and down-regulated. A Venn diagram, created using the VennDiagram *R* package (v1.6.7), depicted the number of significantly responsive genes in both rat strains at $q < 0.05$ (Chen and Boutros 2011). A heatmap gave a visual representation of the change in gene expression, up- versus down-regulation, for the most variable genes (variance >0.05 across all samples). Data was mean centred and scaled using the standard deviation for each variable and clustered as described above. Dotmaps were used to depict the magnitude of change in $\log_2$-space (M) and significance of TCDD-induced dysregulation for different subsets of genes. Covariates were used to indicate significance of selected genes in other tissues and species (rat liver (Yao et al., 2012) and in mouse tissues (Boutros et al., 2009)).

2.7. Pathway analysis of TCDD-responsive genes

Functional pathways analysis was performed with the GOMiner software (v. 2011–01) (Zeeberg et al., 2003). Genes found to be significantly responsive in either strain examined (*q*-value <0.1)

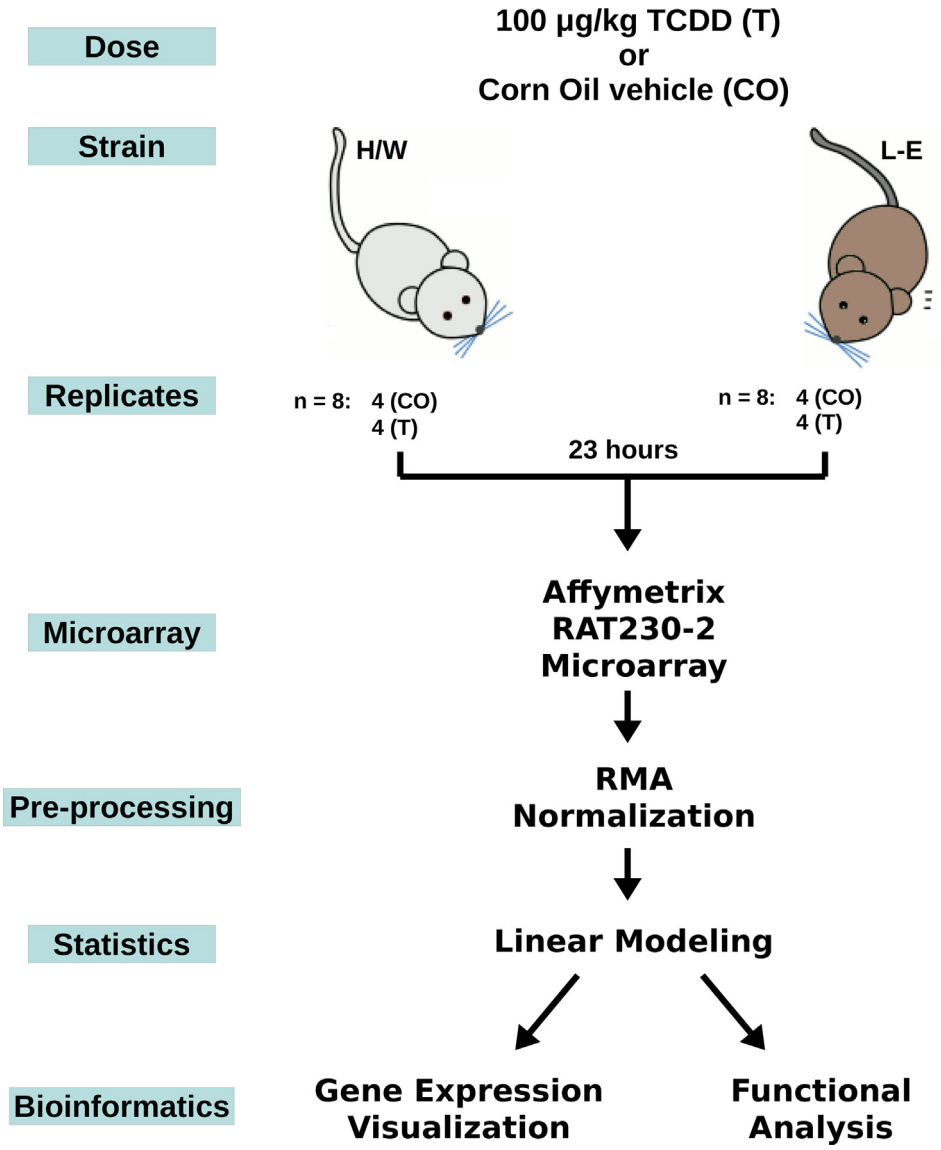

Fig. 1. Experimental design.
Han/Wistar (H/W) and Long–Evans (L–E) rats were evaluated 23 h after treatment with either 100 µg/kg of TCDD (T) or corn oil vehicle (CO). mRNA abundances were measured on Affymetrix Rat Genome 230 2.0 arrays and RMA-normalized prior to downstream analysis.

were analyzed against a list of all genes on the array. A false-discovery rate threshold of 0.1 was applied, with all look-up options and gene ontologies selected and 1000 randomizations used. A minimum category size of five was required to reduce multiple-testing.

2.8. Transcription factor binding site analysis

To further explore the functionality of gene regulation by TCDD in the hypothalamus, we examined each gene for the AHR-associated conserved transcription-factor binding sites: AHRE-I (core), AHRE-I (full) and AHRE-II. These sites contain the sequences GCGTG, [T|G]NGCGTG[A|C][G|C]A and CATG{N6}C[T|A]TG, respectively (Denison and Whitlock 1995; Sogawa et al., 2004). Transcription start sites were determined using REFLINK and REFFLAT tables from UCSC genome browser, downloaded on May 9, 2012 (Karolchik et al., 2003). The number of each motif present in each gene was counted and a PhyloHMM conservation score was calculated, ranging from zero to one (Siepel and Haussler 2004). This score measured conservation across species with a score a zero reflecting minimal conservation and a score of one reflecting complete conservation.

2.9. Validation

A subset of 50 transcripts including the AHR-core and candidate genes (as identified above) was validated using the NanoString system. Hypothalamic RNA (≥100 ng) was shipped on dry ice to the Princess Margaret Genomics Centre (Toronto, ON) for analysis. The target gene list was submitted in advance and the required CodeSet (multiplexed set of endogenous and control probes) was developed by NanoString.

Raw data (RCC files consisting of direct molecule counts) were received and normalization performed prior to analysis. Data were read into the *R* statistical environment (v3.1.2) and normalization performed using the NanoStringNorm package (v1.1.18)(Waggott et al., 2012). Endogenous probes were normalized to the positive control counts using the 'sum' method and to housekeeping genes counts using the 'housekeeping.geo.mean' method in NanoStringNorm. Housekeeping genes (*Hprt1*,*Pgk1* and *Sdha*) had been

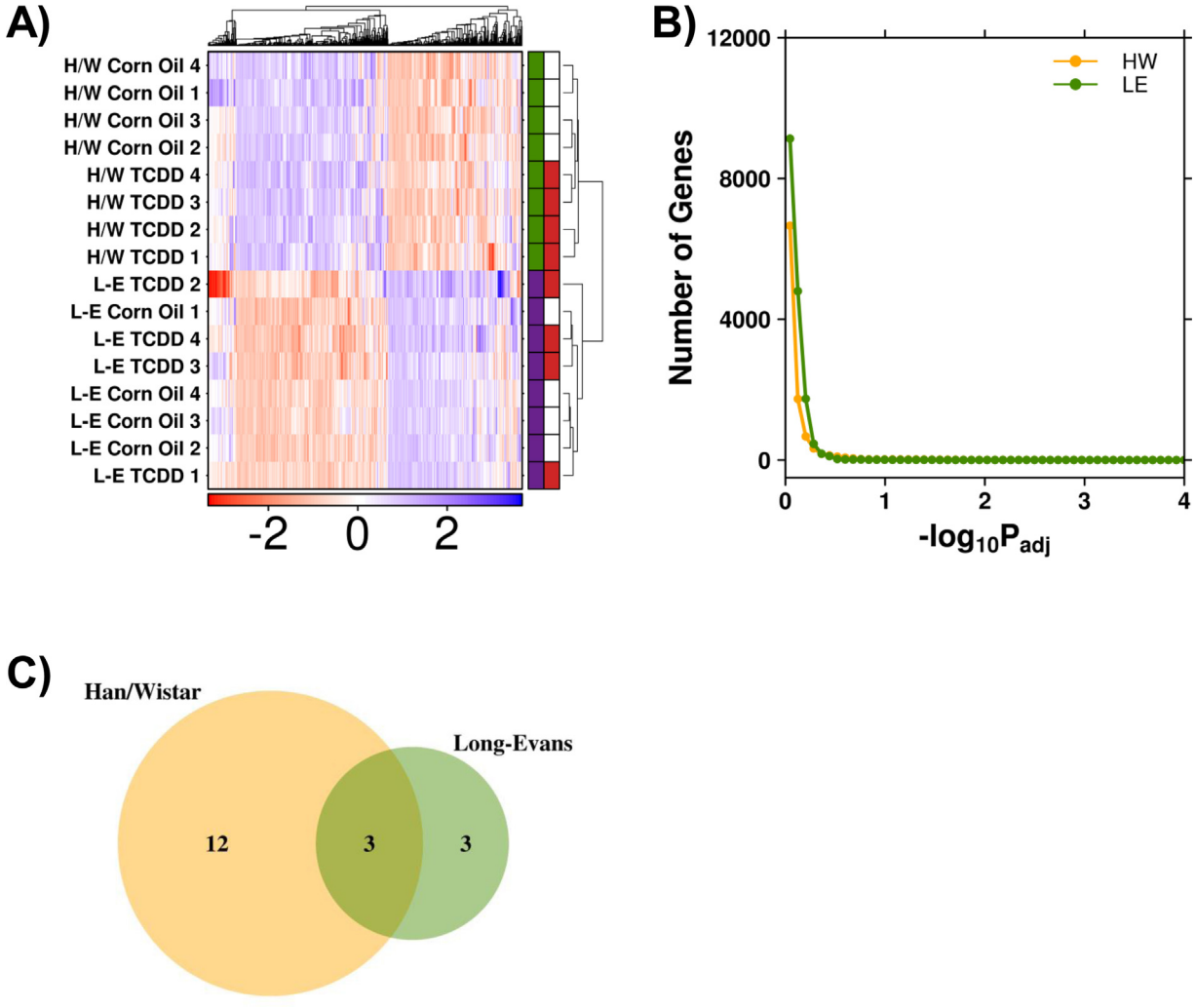

Fig. 2. Strain variability. (For interpretation of the references to colour in this figure legend, the reader is referred to the web version of this article.)
(A) Transcriptomic expression profiles of a subset of genes with the greatest variance (variance >0.05) across the study were subjected to DIANA agglomerative hierarchical clustering. Covariates specify either rat strain (H/W and L–E; green and purple, respectively) or treatment status (TCDD or corn oil control; red or white, respectively). Clustering indicates greater variability in expression profiles between rat strains than between treatment groups. (B) An analysis of the number of genes significantly altered by TCDD at various *q*-value thresholds demonstrate a minimal number of significantly altered genes in either strain (both up- and down-regulated). (C) Overlap of significantly altered genes with a 0.05 *q*-value threshold. Three genes were significantly altered in only L–E rats while 12 genes showed significantly altered expression in only H/W rats. Three genes were found to be significantly differentially expressed in both rat strains.

validated previously (Pohjanvirta et al., 2006) for use in TCDD studies of rat hypothalamus. Similarly, this normalization method had been previously identified as the most accurate (in comparison to qPCR) for use in a similar study with rat hepatic tissue (Prokopec et al., 2013). Normalized data was $\log_2$-transformed and linear modelling and visualizations performed as above [*R* packages: limma (v3.20.9), lattice (v0.20–29), latticeExtra (v0.6–26)].

3. Results

3.1. Experimental design

Since the hypothalamus is associated with the regulation of food intake and metabolism, the effects of TCDD exposure on the hypothalamic transcriptome were analyzed. Two rat strains were examined: TCDD-sensitive L/E rats and TCDD-resistant H/W rats. Animals were treated with 100 μg/kg TCDD or corn oil vehicle. In L–E rats this dose of leads to an irreversible hypophagia and body weight loss, with food intake plummeting from approximately 20 g/day to 1–2 g/day. this rapid decrease in food intake occurred within 5 days of TCDD exposure and thereafter persisted at that level. In contrast in H/W rats, food intake diminishes from slightly above 20 to about 10 g/day 6 days post-treatment, followed by a rapid recovery to near control levels after 14 days (Lensu et al., 2011a). In L–E rats, the reduction in food consumption reaches statistical significance by 24–48 h (Lensu et al., 2011a). Therefore, hypothalamus tissue was isolated 23 h post exposure to identify primary transcriptional changes preceding hypophagia and body weight loss. Moreover, tissues were collected near the end of the darkness period because this phase coincides with one of the two feeding peaks of L–E rats (Lensu et al., 2011b): we thus aimed to optimize the probability of detecting critical alterations. In contrast, at this time of day the circadian feeding rhythm of H/W rats is approaching its nadir (Lensu et al., 2011b). The experimental approach is summarized in Fig. 1. Animals and arrays used are listed in Supplementary Table 1.

Supplementry material related to this article found, in the online version, at http://dx.doi.org/10.1016/j.tox.2014.12.016.

3.2. Response to TCDD Exposure

Normalized microarray data demonstrated very similar mRNA abundances, with hierarchical clustering recognizing greater variability between rat strains than between samples treated with TCDD or corn oil (Fig. 2A). This result suggests that in hypothalamus, unlike liver (Yao et al., 2012), inter-animal variability is larger than the effects of TCDD exposure. Further, the distribution of gene-wise coefficients of variation (CV = ratio of the standard-deviation to mean) shows a strong peak around 0.10 (Supplementary Fig. S2) for each treatment group. There was no evidence of differential variance between the rat strains, with only 15/12,503 genes showing differences (*F*-test; $q < 0.05$). Taken together, these results demonstrate minimal transcriptomic differences between replicates and minimal transcriptomic alterations as a result of TCDD exposure.

Supplementry material related to this article found, in the online version, at http://dx.doi.org/10.1016/j.tox.2014.12.016.

A total of 12,503 individual genes were evaluated (Supplementary Table S2). Surprisingly, a larger number of genes were dysregulated in TCDD-resistant H/W rats than in TCDD-sensitive L–E rats, independent of statistical threshold applied (Fig. 2B). At a standard threshold of $q < 0.05$, we detected 15 genes dysregulated by TCDD in H/W rats and 6 in L–E rats. Only 3 genes, *Cyp1a1*, *Nqo1* and *Stab1*, were altered in both strains (Fig. 2C).

Supplementry material related to this article found, in the online version, at http://dx.doi.org/10.1016/j.tox.2014.12.016.

3.3. AHR-core gene responses

A set of nine genes that are altered by TCDD in an AHR-dependent fashion across a broad range of tissues, species, doses and time-points were assembled (Boutros et al., 2008; Nebert et al., 1993, 2000; Watson et al., 2014; Yeager et al., 2009). These genes (*Ahrr, Aldh3a1, Cyp1a1, Cyp1a2, Fmo1, Inmt, Nfe2l2, Nqo1* and *Tiparp*) provide a measure of the sensitivity of the hypothalamus to transcriptional dysregulation by TCDD, as their effects in other tissues have been well documented. Of these, *Cyp1a1* was significantly up-regulated in both species (3.9-fold in H/W and 3.6-fold in L–E), as was *Nqo1*, though to a lesser extent (0.8-fold in H/W rats and 0.7-fold in L–E). The remaining genes did not show TCDD-induced alteration, despite *Cyp1a2* having previously shown to be upregulated by TCDD in the hypothalamus (Korkalainen et al., 2005). Note that hepatic studies in rats involving similar conditions (100 μg/kg of TCDD, 19 h post-exposure) in both L–E and H/W rats (Yao et al., 2012) demonstrated significantly more TCDD-mediated changes in this subset of genes (Fig. 3A). Similarly, murine studies of liver and kidney tissue following comparable treatment conditions (1000 μg/kg of TCDD, 19 h) (Boutros et al., 2009), showed considerably more TCDD-mediated transcriptional changes (Fig. 3A).

3.4. Non-core gene responses

A subset of genes determined to be significantly altered by TCDD in either strain was identified and further examined. AHR-core genes were excluded from this subset, resulting in 16 genes. These genes exhibited only moderate magnitude dysregulation following TCDD-exposure (Fig. 3B). *Stab1* showed the largest up-regulation amongst non-core genes (1.0-fold induction in the H/W rat) while *Ero1l* showed the greatest down-regulation (H/W, −0.7-fold change). Intriguingly, none of the genes within this subset showed transcriptional dysregulation by TCDD in rat liver, mouse liver or mouse kidney (Boutros et al., 2009; Yao et al., 2012).

3.5. Validation of TCDD-responsive genes

A full validation experiment was performed using a NanoString custom gene expression assay, including both AHR-core and candidate genes. An increased response to TCDD for both strains was observed across the AHR-core genes in the validation relative to the microarray data (Fig. 4, top panel). Both *Cyp1a1* and *Nqo1* showed similar induction, however additional genes were also determined as significantly differentially abundant, including *Cyp1a2* and *Cyp1b1* in both strains and *Aldh3a1* and *Tiparp* in only H/W rats. Conversely, fewer candidate genes were determined to be altered by TCDD in either strain with only 20/32 cases validating (Fig. 4, bottom panel). Of these, *Stab1*, *LOC100361558*, *Ctgf*, *Tmem63a*, and *Hspb9* could be validated in both strains.

3.6. Functional analysis and hypergeometric testing

Functional analysis of those genes showing a significant response to TCDD was completed with the GOMiner software (Zeeberg et al., 2003). No significantly enriched pathways were detected following FDR correction ($q < 0.1$; Supplementary Table S3). Hypergeometric testing was performed to determine if there was chromosomal bias represented in the significantly responsive genes (Supplementary Table S4). No chromosomes were significantly enriched, indicating no chromosomal bias for responses to TCDD in hypothalamus.

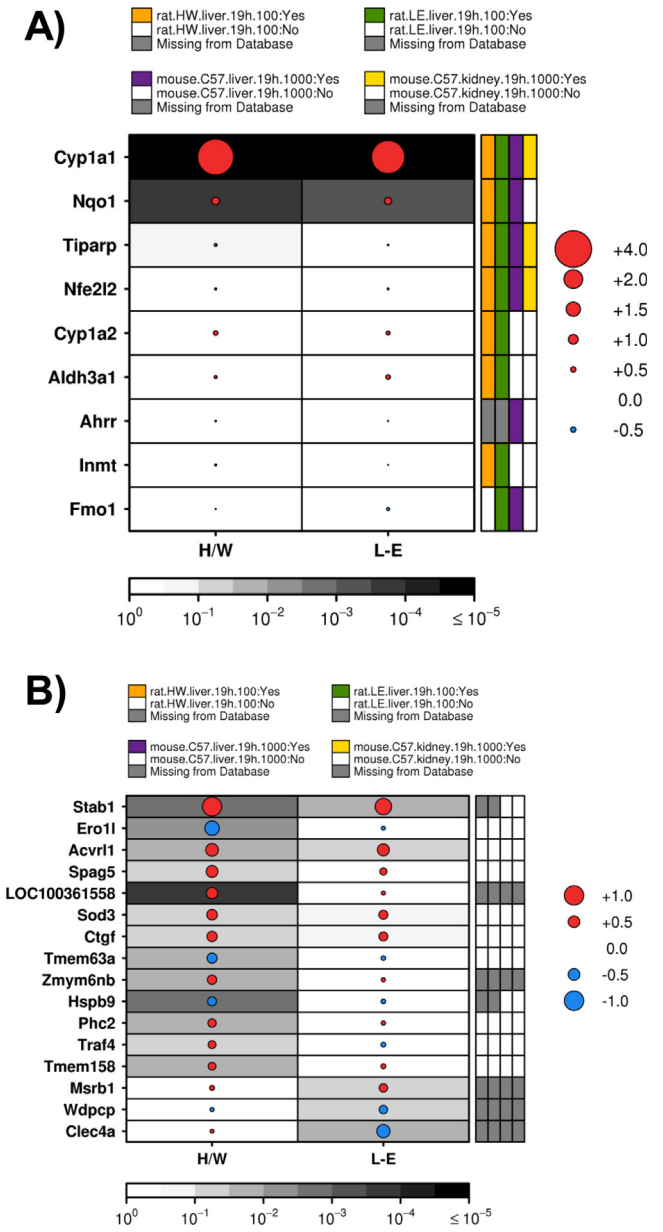

Fig. 3. Gene response to TCDD exposure. (For interpretation of the references to colour in this figure legend, the reader is referred to the web version of this article.) (A) Nine genes within the AHR-core genes were analyzed for their response to TCDD in hypothalamus. The size of the dot depicts the magnitude of the change ($\log_2$ fold change) while colour depicts the direction of change – up (red) or down (blue). Background shading reflects the q-value. Covariates convey whether the gene is significantly expressed in H/W or L–E liver and C57BL/6 mouse kidney or liver. (B) 16 genes outside of the AHR-core were significantly altered by TCDD either H/W ($n = 15$) and/or L–E ($n = 6$). The figure shows the $\log_2$ fold-change values with their corresponding q-value and covariates as described in Fig. 3A. None of these genes were significantly altered in H/W rat liver, L–E rat liver, mouse liver, or mouse kidney.

Supplementry material related to this article found, in the online version, at http://dx.doi.org/10.1016/j.tox.2014.12.016.

3.7. Transcription factor binding site analysis

AHR conserved transcription factor binding site motifs may give further mechanistic insight into the AHR-regulation of genes (Denison and Whitlock 1995; Sogawa et al., 2004). Violin plots (Supplementary Fig. S3) show the occurrence and maximal conservation score of each motif against the number of strains in which the gene was found to be significantly responsive to TCDD exposure (AHRE-I (core), AHRE-I (full) and AHRE-II). AHRE-I (core) was found to occur more often and with higher conservation in genes significantly responsive in both rat strains (*i.e. Cyp1a1* and *Nqo1*). By contrast, AHRE-II was not enriched at either the level of conservation or frequency.

Supplementry material related to this article found, in the online version, at http://dx.doi.org/10.1016/j.tox.2014.12.016.

4. Discussion

The hypothalamic arcuate nucleus (ARC) plays a pivotal role in the regulation of energy balance (Linden et al., 2010). The ARC responds to insulin and leptin signals originating from the periphery and acts via production and release of orexigenic or anorexigenic neuropeptides and hormones and therefore could play an important role in wasting syndrome. Previous studies have indicated that the hypothalamus plays a role in cachexia (Ihnatko et al., 2013) and hypothalamic injury can lead to hyperplasia (Elmquist et al., 1999; Wang et al., 2013). To better understand the role the hypothalamus may play in TCDD-induced wasting syndrome, we analyzed transcriptomic changes occurring in the hypothalamus following TCDD exposure.

mRNA abundance for two of the AHR-core genes, *Cyp1a1* and *Nqo1*, displayed significantly increased abundance following treatment with TCDD. While the magnitude of *Cyp1a1* induction was dramatically lower than that observed in hepatic tissue of similarly treated rats (Yao et al., 2012), levels reached similar abundances as those observed previously in the hypothalamus (Korkalainen et al., 2005). The reduced magnitude of induction of *Nqo1* in hypothalamus relative to liver following TCDD exposure (as observed by both microarray and NanoString) is an interesting finding that has not been reported previously. Alternatively, the absence of significant Cyp1a2 induction following treatment may be an artifact of the array technology as significant induction resembling that observed previously (Korkalainen et al., 2005) was validated by NanoString in these samples.

With the exception of *Cyp1a1*, altered genes exhibited only modest changes in abundance in response to TCDD, with changes of less than two-fold relative to control animals. This low magnitude of change in candidate genes was similarly observed by NanoString validation. The relatively few alterations to the transcriptome, combined with the small magnitude of these changes may suggest that the hypothalamus is largely refractory to direct local effects of TCDD. However, the specific genes showing significant alterations may still shed evidence on downstream toxicities. A group of 3 genes were significantly altered only in L-E rats and may therefore be involved in the sensitive phenotype. MSRB1 is involved in the protein repair mechanism during oxidative stress (Lee et al., 2009) and has been shown to regulate assembly of actin filaments relating to macrophage activity (Lee et al., 2013). Increased abundance of this mRNA may indicate a potential defense mechanism against TCDD-induced reactive oxygen species. Alternatively, decreased mRNA abundances of *Wdpcp* and *Clec4a* may have etiological roles in TCDD-induced toxicity. *Wdpcp* is required for the stabilization of actin filaments and development of cell polarity (Cui et al., 2013) while *Clec4a* (DCIR) is typically expressed in immune tissues (Bates et al., 1999) and is involved in the immune response.

Of the 11 genes uniquely altered in H/W rats, nine were up-regulated by TCDD while the remaining three were down-regulated. *Ctgf* has been validated as an AHR-target gene coding for CTGF, a regulatory protein that mediates cell division and apoptosis and has been documented to promote tumour growth

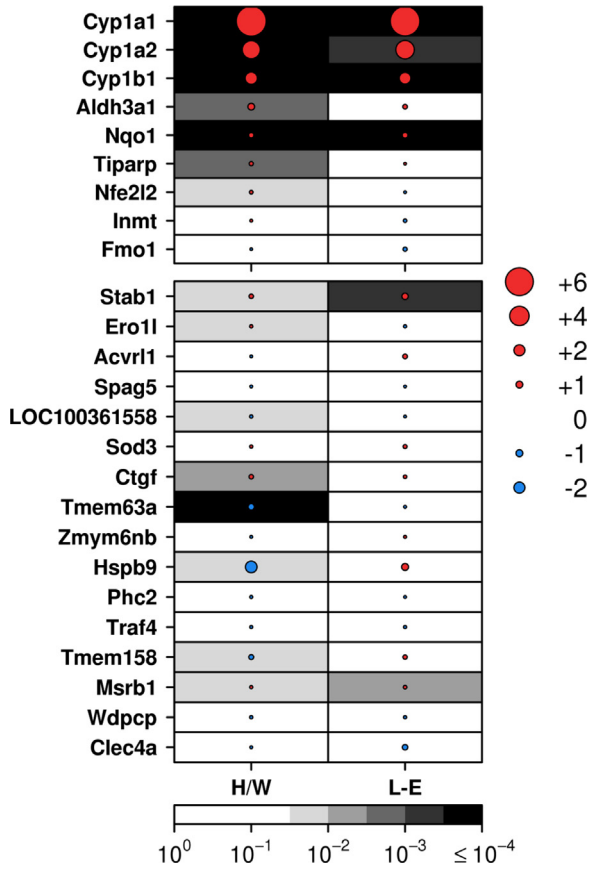

Fig. 4. Validation of candidate genes. (For interpretation of the references to colour in this figure legend, the reader is referred to the web version of this article.) Validation was performed on 9 AHR-core genes and 16 candidate genes. The size of the dot depicts the magnitude of the change ($\log_2$ fold change) while colour depicts the direction of change – up (red) or down (blue). Background shading reflects the *q*-value.

and progression (Chu et al., 2008; Faust et al., 2013). It also plays an important role in mediating cell adhesion and migration primarily in activation of rat oval cells (Pi et al., 2008). *Sod3* has been shown to act as a tumour suppressor in prostate (Kim et al., 2014) and pancreatic cancer (Sibenaller et al., 2014) by modulation of ROS. Alternatively, induction of *Ero1l* by HIF-1α within a hypoxic microenvironment leads to angiogenesis and improved tumour survival (May et al., 2005). Within the resistant H/W strain, these findings (overexpression of *Sod3* and reduced expression of *Ero1l*) align with the reduced carcinogenic effects of TCDD. *Traf4* is a common oncogene (Camilleri-Broet et al., 2007), however overexpression has also been shown to be essential for homeostasis of CNS myelination (Blaise et al., 2012).

Two genes, *Stab1* and *Acvrl1*, were overexpressed in both H/W and L–E rats. STAB1 is a scavenger receptor expressed by macrophages and may aid in phagocytic and anti-inflammatory processes (Park et al., 2009). ACVRL1 is a type 1 receptor for TGF-beta proteins and is required for angiogenesis (Oh et al., 2000). Increased mRNA abundance of these genes may represent a common adaptive response to TCDD-induced damages.

Previous studies comparing mRNA abundance changes following TCDD treatment have shown L–E rats have significantly higher numbers of genes dysregulated by TCDD, as compared to H/W rat (Franc et al., 2008; Yao et al., 2012). However, the hypothalamus of H/W rats had more altered transcripts than in L–E rats. Given that all animals from both rat strains had reached sexual maturity at the time of TCDD exposure, it is not likely that the difference in age affected the transcriptomic response. Similarly, animals experienced identical environmental and handling conditions. Although the magnitude of *Cyp1a1* induction is low in hypothalamus when compared with liver, the observed induction in both L–E and H/W rats indicates that TCDD does in fact reach and effectively activate theAHR in the hypothalamus of both strains, in accordance with previous work (Pohjanvirta et al., 1990). It is important to note that our study was designed to emphasize detection of early transcriptomic responses during the time when the onset of measurable feeding responses occurs in TCDD-treated rats.

A study conducted by Linden et al. (2005) on the effect of TCDD exposure on neuropeptide concentrations further supports our results as it showed that TCDD alters anorexigenic and orexigenic neuropeptides but not consistently (Linden et al., 2005). Attention has now turned to nitric oxide and its combined effects with orexigenic peptides, ghrelin, NPY and orexin-A, in food intake regulation. An alteration in nitric oxide concentration may indirectly affect this regulatory pathway, although results of these studies have not been conclusive (Linden et al., 2010). Ventromedial hypothalamic lesions aggravate TCDD-induced weight loss and, therefore, indicate that TCDD implements toxic effects at some point along the hypothalamic pathways regulating energy homeostasis (Tuomisto et al., 1995). The minimal impact of TCDD on hypothalamic transcriptomic responses in hypothalamus seen in this study, along with studies on TCDD response of mRNAs for hypothalamic neuropeptides and *bHLS/PAS* proteins, suggest that hypothalamic changes alone are not responsible for TCDD-induced hypophagia (Korkalainen et al., 2005; Linden et al., 2005). Analysis of the entire hypothalamic tissue block may mask strictly localized alterations in functionally-specific nuclei.

The hypothalamus is a highly compartmentalized structure consisting of clusters of functionally specialized cells (Schindler et al., 2012), each type of which could have diverse responses to TCDD. The tissue samples we analyzed are derived from the whole hypothalamus. An in depth analysis of specialized cell types might provide more enlightening results. Alternatively, the hypothalamus may be indirectly involved in wasting-syndrome-associated hypophagia as TCDD may directly affect other feed-intake regulatory organs. Analysis of alternate nervous system components in this regulatory pathway (*i.e.* caudal brainstem and medullary area postrema) as well as factors upstream or downstream (*i.e.* adipose tissue) may provide more insight into the mechanisms underlying toxic effects of TCDD, as they pertain to wasting syndrome.

Authors' contributions

Animal work: RP, JL, SL; sample preparation: IDM, RP, SDP bioinformatics analysis: KEH, SDP, PCB; wrote the first draft of the manuscript: KEH; initiated the project: ABO, RP; supervised research: ABO, RP, PCB; generated tools and reagents: SDP; approved the manuscript: all authors.

Conflict of interest

ABO has served as a paid consultant to the Dow Chemical Company as a member of their Dioxin Scientific Advisory Board. All other authors declare that they have no conflicts of interest.

Funding sources

This work was supported by the Canadian Institutes of Health Research (grant number MOP-57903 to ABO and PCB), the Academy of Finland (grant numbers 123345 and 261232 to RP) and with the support of the Ontario Institute for Cancer Research to

PCB through funding provided by the Government of Ontario. PCB was supported by a CIHR New Investigator Award. The study sponsors had no role in the study design; in the collection, analysis and interpretation of data; in the writing of the report; or in the decision to submit the paper for publication.

Transparency document

The Transparency document associated with this article can be found in the online version.

Acknowledgements

The authors thank all members of the Boutros lab for helpful suggestions.

Reference

Bates, E.E., Fournier, N., Garcia, E., Valladeau, J., Durand, I., Pin, J.J., Zurawski, S.M., Patel, S., Abrams, J.S., Lebecque, S., Garrone, P., Saeland, S., 1999. APCs express DCIR, a novel C-type lectin surface receptor containing an immunoreceptor tyrosine-based inhibitory motif. J. Immunol. 163, 1973–1983.

Blaise, S., Kneib, M., Rousseau, A., Gambino, F., Chenard, M.P., Messadeq, N., Muckenstrum, M., Alpy, F., Tomasetto, C., Humeau, Y., Rio, M.C., 2012. In vivo evidence that TRAF4 is required for central nervous system myelin homeostasis. PLoS One 7, e30917.

Boutros, P.C., Bielefeld, K.A., Pohjanvirta, R., Harper, P.A., 2009. Dioxin-dependent and dioxin-independent gene batteries: comparison of liver and kidney in AHR-null mice. Toxicol. Sci. 112, 245–256.

Boutros, P.C., Yan, R., Moffat, I.D., Pohjanvirta, R., Okey, A.B., 2008. Transcriptomic responses to 2,3,7,8-tetrachlorodibenzo-p-dioxin (TCDD) in liver: comparison of rat and mouse. BMC Genomics 9, 419.

Boutros, P.C., Yao, C.Q., Watson, J.D., Wu, A.H., Moffat, I.D., Prokopec, S.D., Smith, A.B., Okey, A.B., Pohjanvirta, R., 2011. Hepatic transcriptomic responses to TCDD in dioxin-sensitive and dioxin-resistant rats during the onset of toxicity. Toxicol. Appl. Pharmacol. 251, 119–129.

Camilleri-Broet, S., Cremer, I., Marmey, B., Comperat, E., Viguie, F., Audouin, J., Rio, M. C., Fridman, W.H., Sautes-Fridman, C., Regnier, C.H., 2007. TRAF4 overexpression is a common characteristic of human carcinomas. Oncogene 26, 142–147.

Chen, H., Boutros, P.C., 2011. VennDiagram: a package for the generation of highly-customizable Venn and Euler diagrams in R. BMC Bioinf. 12, 35.

Chu, C.Y., Chang, C.C., Prakash, E., Kuo, M.L., 2008. Connective tissue growth factor (CTGF) and cancer progression. J. Biomed. Sci. 15, 675–685.

Cui, C., Chatterjee, B., Lozito, T.P., Zhang, Z., Francis, R.J., Yagi, H., Swanhart, L.M., Sanker, S., Francis, D., Yu, Q., San Agustin, J.T., Puligilla, C., Chatterjee, T., Tansey, T., Liu, X., Kelley, M.W., Spiliotis, E.T., Kwiatkowski, A.V., Tuan, R., Pazour, G.J., Hukriede, N.A., Lo, C.W., 2013. Wdpcp, a PCP protein required for ciliogenesis, regulates directional cell migration and cell polarity by direct modulation of the actin cytoskeleton. PLoS Biol. 11, e1001720.

Dai, M., Wang, P., Boyd, A.D., Kostov, G., Athey, B., Jones, E.G., Bunney, W.E., Myers, R. M., Speed, T.P., Akil, H., Watson, S.J., Meng, F., 2005. Evolving gene/transcript definitions significantly alter the interpretation of GeneChip data. Nucleic Acids Res. 33, e175.

Denison, M.S., Whitlock Jr., J.P., 1995. Xenobiotic-inducible transcription of cytochrome *P450* genes. J. Biol. Chem. 270, 18175–18178.

Dolwick, K.M., Schmidt, J.V., Carver, L.A., Swanson, H.I., Bradfield, C.A., 1993. Cloning and expression of a human Ah receptor cDNA. Mol. Pharmacol. 44, 911–917.

Elmquist, J.K., Elias, C.F., Saper, C.B., 1999. From lesions to leptin: hypothalamic control of food intake and body weight. Neuron 22, 221–232.

Faust, D., Vondracek, J., Krcmar, P., Smerdova, L., Prochazkova, J., Hruba, E., Hulinkova, P., Kaina, B., Dietrich, C., Machala, M., 2013. AhR-mediated changes in global gene expression in rat liver progenitor cells. Arch. Toxicol. 87, 681–698.

Franc, M.A., Moffat, I.D., Boutros, P.C., Tuomisto, J.T., Tuomisto, J., Pohjanvirta, R., Okey, A.B., 2008. Patterns of dioxin-altered mRNA expression in livers of dioxin-sensitive versus dioxin-resistant rats. Arch. Toxicol. 82, 809–830.

Gautier, L., Cope, L., Bolstad, B.M., Irizarry, R.A., 2004. Affy–analysis of Affymetrix GeneChip data at the probe level. Bioinformatics 20, 307–315.

Ihnatko, R., Post, C., Blomqvist, A., 2013. Proteomic profiling of the hypothalamus in a mouse model of cancer-induced anorexia-cachexia. Br. J. Cancer 109, 1867–1875.

Irizarry, R.A., Bolstad, B.M., Collin, F., Cope, L.M., Hobbs, B., Speed, T.P., 2003. Summaries of Affymetrix GeneChip probe level data. Nucleic Acids Res. 31, e15.

Karolchik, D., Baertsch, R., Diekhans, M., Furey, T.S., Hinrichs, A., Lu, Y.T., Roskin, K.M., Schwartz, M., Sugnet, C.W., Thomas, D.J., Weber, R.J., Haussler, D., Kent, W.J., 2003. The UCSC Genome Browser Database. Nucleic Acids Res. 31, 51–54.

Kilkenny, C., Browne, W.J., Cuthill, I.C., Emerson, M., Altman, D.G., 2010. Improving bioscience research reporting: the ARRIVE guidelines for reporting animal research. PLoS Biol. 8, e1000412.

Kim, J., Mizokami, A., Shin, M., Izumi, K., Konaka, H., Kadono, Y., Kitagawa, Y., Keller, E.T., Zhang, J., Namiki, M., 2014. SOD3 acts as a tumor suppressor in PC-3 prostate cancer cells via hydrogen peroxide accumulation. Anticancer Res. 34, 2821–2831.

Ko, H.P., Okino, S.T., Ma, Q., Whitlock Jr., J.P., 1997. Transactivation domains facilitate promoter occupancy for the dioxin-inducible *CYP1A1* gene in vivo. Mol. Cell Biol. 17, 3497–3507.

Konner, A.C., Klockener, T., Bruning, J.C., 2009. Control of energy homeostasis by insulin and leptin: targeting the arcuate nucleus and beyond. Physiol. Behav. 97, 632–638.

Korkalainen, M., Linden, J., Tuomisto, J., Pohjanvirta, R., 2005. Effect of TCDD on mRNA expression of genes encoding bHLH/PAS proteins in rat hypothalamus. Toxicology 208, 1–11.

Lee, B.C., Dikiy, A., Kim, H.Y., Gladyshev, V.N., 2009. Functions and evolution of selenoprotein methionine sulfoxide reductases. Biochim. Biophys. Acta 1790, 1471–1477.

Lee, B.C., Peterfi, Z., Hoffmann, F.W., Moore, R.E., Kaya, A., Avanesov, A., Tarrago, L., Zhou, Y., Weerapana, E., Fomenko, D.E., Hoffmann, P.R., Gladyshev, V.N., 2013. MsrB1 and MICALs regulate actin assembly and macrophage function via reversible stereoselective methionine oxidation. Mol. Cell 51, 397–404.

Lensu, S., Tiittanen, P., Linden, J., Tuomisto, J., Pohjanvirta, R., 2011a. Effects of a single exposure to 2,3,7,8-tetrachlorodibenzo-ρ-dioxin (TCDD) on macro- and microstructures of feeding and drinking in two differently TCDD-sensitive rat strains. Pharmacol. Biochem. Behav. 99, 487–499.

Lensu, S., Tiittanen, P., Pohjanvirta, R., 2011b. Circadian differences between two rat strains in their feeding and drinking micro- and macrostructures. Biol. Rhythm Res. 42, 385–405.

Linden, J., Korkalainen, M., Lensu, S., Tuomisto, J., Pohjanvirta, R., 2005. Effects of 2,3,7,8-tetrachlorodibenzo-ρ-dioxin (TCDD) and leptin on hypothalamic mRNA expression of factors participating in food intake regulation in a TCDD-sensitive and a TCDD-resistant rat strain. J. Biochem. Mol. Toxicol. 19, 139–148.

Linden, J., Lensu, S., Pohjanvirta, R., 2014. Effect of 2,3,7,8-tetrachlorodibenzo-ρ-dioxin (TCDD) on hormones of energy balance in a TCDD-sensitive and a TCDD-resistant rat strain. Int. J. Mol. Sci. 15, 13938–13966.

Linden, J., Lensu, S., Tuomisto, J., Pohjanvirta, R., 2010. Dioxins, the aryl hydrocarbon receptor and the central regulation of energy balance. Front. Neuroendocrinol. 31, 452–478.

May, D., Itin, A., Gal, O., Kalinski, H., Feinstein, E., Keshet, E., 2005. Ero1-L alpha plays a key role in a HIF-1-mediated pathway to improve disulfide bond formation and VEGF secretion under hypoxia: implication for cancer. Oncogene 24, 1011–1020.

Mimura, J., Fujii-Kuriyama, Y., 2003. Functional role of AhR in the expression of toxic effects by TCDD. Biochim. Biophys. Acta 1619, 263–268.

Moffat, I.D., Roblin, S., Harper, P.A., Okey, A.B., Pohjanvirta, R., 2007. Aryl hydrocarbon receptor splice variants in the dioxin-resistant rat: tissue expression and transactivational activity. Mol. Pharmacol. 72, 956–966.

Nebert, D.W., Puga, A., Vasiliou, V., 1993. Role of the Ah receptor and the dioxin-inducible [Ah] gene battery in toxicity, cancer, and signal transduction. Ann, N, Y, Acad, Sci. 685, 624–640.

Nebert, D.W., Roe, A.L., Dieter, M.Z., Solis, W.A., Yang, Y., Dalton, T.P., 2000. Role of the aromatic hydrocarbon receptor and [Ah] gene battery in the oxidative stress response, cell cycle control, and apoptosis. Biochem. Pharmacol. 59, 65–85.

Oh, S.P., Seki, T., Goss, K.A., Imamura, T., Yi, Y., Donahoe, P.K., Li, L., Miyazono, K., ten Dijke, P., Kim, S., Li, E., 2000. Activin receptor-like kinase 1 modulates transforming growth factor-beta 1 signaling in the regulation of angiogenesis. Proc. Natl. Acad. Sci. U. S. A. 97, 2626–2631.

Okey, A.B., 2007. An aryl hydrocarbon receptor odyssey to the shores of toxicology: the deichmann lecture, international congress of toxicology-XI. Toxicol. Sci. 98, 5–38.

Park, S.Y., Jung, M.Y., Lee, S.J., Kang, K.B., Gratchev, A., Riabov, V., Kzhyshkowska, J., Kim, I.S., 2009. Stabilin-1 mediates phosphatidylserine-dependent clearance of cell corpses in alternatively activated macrophages. J. Cell Sci. 122, 3365–3373.

Petrulis, J.R., Perdew, G.H., 2002. The role of chaperone proteins in the aryl hydrocarbon receptor core complex. Chem. Biol. Interact 141, 25–40.

Pi, L., Ding, X., Jorgensen, M., Pan, J.J., Oh, S.H., Pintilie, D., Brown, A., Song, W.Y., Petersen, B.E., 2008. Connective tissue growth factor with a novel fibronectin binding site promotes cell adhesion and migration during rat oval cell activation. Hepatology 47, 996–1004.

Pohjanvirta, R., Niittynen, M., Linden, J., Boutros, P.C., Moffat, I.D., Okey, A.B., 2006. Evaluation of various housekeeping genes for their applicability for normalization of mRNA expression in dioxin-treated rats. Chem. Biol. Interact 160, 134–149.

Pohjanvirta, R., Tuomisto, J., 1994. Short-term toxicity of 2,3,7,8-tetrachlorodibenzo-ρ-dioxin in laboratory animals: effects, mechanisms, and animal models. Pharmacol. Rev. 46, 483–549.

Pohjanvirta, R., Unkila, M., Linden, J., Tuomisto, J.T., Tuomisto, J., 1995. Toxic equivalency factors do not predict the acute toxicities of dioxins in rats. Eur. J. Pharmacol. 293, 341–353.

Pohjanvirta, R., Vartiainen, T., Uusi-Rauva, A., Monkkonen, J., Tuomisto, J., 1990. Tissue distribution, metabolism, and excretion of 14C-TCDD in a TCDD-susceptible and a TCDD-resistant rat strain. Pharmacol. Toxicol. 66, 93–100.

Pohjanvirta, R., Wong, J.M., Li, W., Harper, P.A., Tuomisto, J., Okey, A.B., 1998. Point mutation in intron sequence causes altered carboxyl-terminal structure in the aryl hydrocarbon receptor of the most 2,3,7,8-tetrachlorodibenzo-ρ-dioxin-resistant rat strain. Mol. Pharmacol. 54, 86–93.

Prokopec, S.D., Watson, J.D., Waggott, D.M., Smith, A.B., Wu, A.H., Okey, A.B., Pohjanvirta, R., Boutros, P.C., 2013. Systematic evaluation of medium-throughput mRNA abundance platforms. RNA 19, 51–62.

Reyes, H., Reisz-Porszasz, S., Hankinson, O., 1992. Identification of the Ah receptor nuclear translocator protein (Arnt) as a component of the DNA binding form of the Ah receptor. Science 256, 1193–1195.
Schindler, S., Geyer, S., Strauss, M., Anwander, A., Hegerl, U., Turner, R., Schonknecht, P., 2012. Structural studies of the hypothalamus and its nuclei in mood disorders. Psychiatry Res. 201, 1–9.
Seefeld, M.D., Corbett, S.W., Keesey, R.E., Peterson, R.E., 1984. Characterization of the wasting syndrome in rats treated with 2,3,7,8-tetrachlorodibenzo-ρ-dioxin. Toxicol. Appl. Pharmacol. 73, 311–322.
Sibenaller, Z.A., Welsh, J.L., Du, C., Witmer, J.R., Schrock, H.E., Du, J., Buettner, G.R., Goswami, P.C., Cieslak 3rd, J.A., Cullen, J.J., 2014. Extracellular superoxide dismutase suppresses hypoxia-inducible factor-1alpha in pancreatic cancer. Free Radical Biol. Med. 69, 357–366.
Siepel, A., Haussler, D., 2004. Combining phylogenetic and hidden Markov models in biosequence analysis. J. Comput. Biol. 11, 413–428.
Smyth, G.K., 2004. Linear models and empirical bayes methods for assessing differential expression in microarray experiments. Stat. Appl. Genet. Mol. Biol. 3, Article3.
Sogawa, K., Numayama-Tsuruta, K., Takahashi, T., Matsushita, N., Miura, C., Nikawa, J., Gotoh, O., Kikuchi, Y., Fujii-Kuriyama, Y., 2004. A novel induction mechanism of the rat *CYP1A2* gene mediated by Ah receptor-Arnt heterodimer. Biochem. Biophys. Res. Commun. 318, 746–755.
Storey, J.D., Tibshirani, R., 2003. Statistical significance for genomewide studies. Proc. Natl. Acad. Sci. U. S. A. 100, 9440–9445.
Tuomisto, J.T., Pohjanvirta, R., Unkila, M., Tuomisto, J., 1995. 2,3,7,8-Tetrachlorodibenzo-ρ-dioxin-induced anorexia and wasting syndrome in rats: aggravation after ventromedial hypothalamic lesion. Eur. J. Pharmacol. 293, 309–317.
Tuomisto, J.T., Pohjanvirta, R., Unkila, M., Tuomisto, J., 1999. TCDD-induced anorexia and wasting syndrome in rats: effects of diet-induced obesity and nutrition. Pharmacol. Biochem. Behav. 62, 735–742.
Unkila, M., Pohjanvirta, R., MacDonald, E., Tuomisto, J.T., Tuomisto, J., 1994. Dose response and time course of alterations in tryptophan metabolism by 2,3,7,8-tetrachlorodibenzo-ρ-dioxin (TCDD) in the most TCDD-susceptible and the most TCDD-resistant rat strain: relationship with TCDD lethality. Toxicol. Appl. Pharmacol. 128, 280–292.
Waggott, D., Chu, K., Yin, S., Wouters, B.G., Liu, F.F., Boutros, P.C., 2012. NanoStringNorm: an extensible R package for the pre-processing of nanoString mRNA and miRNA data. Bioinformatics 28, 1546–1548.
Wang, J., Yuan, Z., Dong, J., Zhang, D., Usami, T., Murata, T., Narita, K., Higuchi, T., 2013. Neuropeptide Y loses its orexigenic effect in rats with lesions of the hypothalamic paraventricular nucleus. Endocr. Res. 38, 8–14.
Watson, J.D., Prokopec, S.D., Smith, A.B., Okey, A.B., Pohjanvirta, R., Boutros, P.C., 2014. TCDD dysregulation of 13 AHR-target genes in rat liver. Toxicol. Appl. Pharmacol. 274, 445–454.
Yao, C.Q., Prokopec, S.D., Watson, J.D., Pang, R., P'ng, C., Chong, L.C., Harding, N.J., Pohjanvirta, R., Okey, A.B., Boutros, P.C., 2012. Inter-strain heterogeneity in rat hepatic transcriptomic responses to 2,3,7,8-tetrachlorodibenzo-ρ-dioxin (TCDD). Toxicol. Appl. Pharmacol. 260, 135–145.
Yeager, R.L., Reisman, S.A., Aleksunes, L.M., Klaassen, C.D., 2009. Introducing the TCDD-inducible *AhR-Nrf2* gene battery. Toxicol. Sci. 111, 238–246.
Zeeberg, B.R., Feng, W., Wang, G., Wang, M.D., Fojo, A.T., Sunshine, M., Narasimhan, S., Kane, D.W., Reinhold, W.C., Lababidi, S., Bussey, K.J., Riss, J., Barrett, J.C., Weinstein, J.N., 2003. GoMiner: a resource for biological interpretation of genomic and proteomic data. Genome Biol. 4, R28.

CellPress

Cell Metabolism
Short Article

Interindividual Variation in DNA Methylation at a Putative *POMC* Metastable Epiallele Is Associated with Obesity

Peter Kühnen,[1,15,16,*] Daniela Handke,[1,15] Robert A. Waterland,[2] Branwen J. Hennig,[3] Matt Silver,[3] Anthony J. Fulford,[3] Paula Dominguez-Salas,[4,5] Sophie E. Moore,[3,6] Andrew M. Prentice,[3] Joachim Spranger,[7,8] Anke Hinney,[9] Johannes Hebebrand,[9] Frank L. Heppner,[10,11] Lena Walzer,[1] Carsten Grötzinger,[12] Jörg Gromoll,[13] Susanna Wiegand,[14] Annette Grüters,[14] and Heiko Krude[1]

[1]Institute for Experimental Pediatric Endocrinology, Charité Universitätsmedizin Berlin, 13353 Berlin, Germany
[2]USDA/ARS Children's Nutrition Research Center, Departments of Pediatrics and Molecular and Human Genetics, Baylor College of Medicine, Houston, TX 77030, USA
[3]MRC Unit, The Gambia and MRC International Nutrition Group, London School of Hygiene and Tropical Medicine, London WC1E 7HT, UK
[4]Veterinary Epidemiology, Economics and Public Health Group, Royal Veterinary College, University of London, Hertfordshire AL10 9EU, UK
[5]International Livestock Research Institute, 00100 Nairobi, Kenya
[6]Elsie Widdowson Laboratory, MRC Human Nutrition Research, Cambridge CB1 9NL, UK
[7]Department of Endocrinology, Diabetes, and Nutrition and Charité Center for Cardiovascular Research (CCR), Charité Universitätsmedizin Berlin, 10117 Berlin, Germany
[8]Experimental and Clinical Research Center (ECRC), Charité Universitätsmedizin Berlin and Max-Delbrück Centre, 10117 Berlin, Germany
[9]Department of Child and Adolescent Psychiatry, University Hospital Essen (AöR), University of Duisburg-Essen, 45141 Essen, Germany
[10]Department of Neuropathology, Charité Universitätsmedizin Berlin, 10117 Berlin, Germany
[11]Cluster of Excellence, NeuroCure, Charitéplatz 1, 10117 Berlin, Germany
[12]Department of Hepatology and Gastroenterology, Molecular Cancer Research Center (MKFZ), Charité Universitätsmedizin Berlin, 13353 Berlin, Germany
[13]Centre of Reproductive Medicine and Andrology, University of Münster, 48149 Münster, Germany
[14]Department of Pediatric Endocrinology and Diabetes, Charité Universitätsmedizin, 13353 Berlin, Germany
[15]Co-first author
[16]Lead Contact
*Correspondence: peter.kuehnen@charite.de
http://dx.doi.org/10.1016/j.cmet.2016.08.001

SUMMARY

The estimated heritability of human BMI is close to 75%, but identified genetic variants explain only a small fraction of interindividual body-weight variation. Inherited epigenetic variants identified in mouse models named "metastable epialleles" could in principle explain this "missing heritability." We provide evidence that methylation in a variably methylated region (VMR) in the pro-opiomelanocortin gene (*POMC*), particularly in postmortem human laser-microdissected melanocyte-stimulating hormone (MSH)-positive neurons, is strongly associated with individual BMI. Using cohorts from different ethnic backgrounds, including a Gambian cohort, we found evidence suggesting that methylation of the *POMC* VMR is established in the early embryo and that offspring methylation correlates with the paternal somatic methylation pattern. Furthermore, it is associated with levels of maternal one-carbon metabolites at conception and stable during postnatal life. Together, these data suggest that the *POMC* VMR may be a human metastable epiallele that influences body-weight regulation.

INTRODUCTION

Family and twin studies indicate that adiposity (assessed as BMI) is highly heritable. A recent meta-analysis estimated BMI heritability up to 75% in twins and 46% in families (Elks et al., 2012). However, despite enormous efforts (Speliotes et al., 2010), including whole-genome sequencing (Yang et al., 2015), the genetic variants identified thus far together explain <30% of individual BMI and body-weight variation (Locke et al., 2015). The last few years have seen efforts to explain this "missing heritability" by exploring the relation between epigenetic modifications and body-weight regulation (Eichler et al., 2010). However, the molecular nature and ontogeny have remained elusive (Waterland, 2014). The most comprehensive search for obesity-related DNA methylation changes in humans based on the Illumina 450K array recently revealed *HIF3A* methylation variants associated with BMI (Dick et al., 2014; Murphy and Mill, 2014). However, as these were linked with SNPs in *cis*, they may represent secondary epigenetic differences that are driven by genetic variation.

The most compelling data supporting epigenetic regulation of body weight/BMI is derived from mouse models identifying changes in DNA methylation and gene expression (Dalgaard et al., 2016; Radford et al., 2014). For example, cloned (Tamashiro et al., 2002) and isogenic inbred (Koza et al., 2006) mouse strains are divergent in their body weight early in life despite sharing the same genomes and environment.

At the molecular level these inherited, stable epigenetic variants were initially shown for fur color and body weight in the agouti viable yellow (A^{vy}) mouse (Morgan et al., 1999). In the A^{vy} mutant strain, epigenetic variants are triggered by a transposable element (intracisternal A particle [IAP]). Methylation of this retrotransposon in the early embryo leads to stable, non-tissue-specific epigenetic variation among isogenic A^{vy} mice that influences fur color and metabolic phenotypes. Accordingly, A^{vy} was dubbed a "metastable epiallele" (ME) (Rakyan et al., 2002). This concept of a retro-element triggered ME was confirmed in the murine $Axin^{Fu}$ mutation, at which interindividual variation in methylation is associated with tail kinking (Rakyan et al., 2002). It was shown that methylation at MEs occurs stochastically but can in part be modified by maternal intake of nutrients related to one-carbon (C1) metabolism (Waterland et al., 2006; Waterland and Jirtle, 2003). In addition, the methylation state can in part be transmitted via a parental germline, either maternal (A^{vy}) (Morgan et al., 1999) or paternal ($Axin^{Fu}$) (Rakyan et al., 2003). Thus, epigenetic differences at metastable epialleles represent a potential molecular mechanism to explain stable inheritance that is not linked to genetic variants.

Here, we pursued a candidate gene approach to identify BMI-associated DNA methylation differences. We focused our search on the *POMC* gene, because individuals homozygous for variants in the coding region of *POMC* (giving rise to the melanocyte-stimulating hormone [MSH] peptides that mediate the anorectic functions of leptin) develop early-onset severe obesity (Krude et al., 1998). Since heterozygous carriers are obese to a lesser extent (Farooqi et al., 2006; Krude et al., 2003), *POMC* represents a good candidate for investigating the potential effects of methylation differences on gene expression and obesity/BMI.

We previously identified a *POMC* variably methylated region (VMR) located at the intron 2/exon 3 border (Figure 1A), which is more frequently hypermethylated in peripheral blood cells (PBCs) of obese children (Kuehnen et al., 2012). Hypermethylation of the VMR seems to be triggered by adjacent Alu elements in intron 2 (Figure 1A), since the homologous CpGs in species without those Alu elements (mouse and lemur) are not methylated. We have shown that hypermethylation in this VMR decreases P300 enhancer binding and *POMC* transcription and is present before the onset of obesity (Kuehnen et al., 2012), suggesting a functional effect of the methylation variant on *POMC* gene expression. Here, we extend our previous study to look at *POMC* methylation in PBCs and MSH neurons in adults.

RESULTS

POMC Hypermethylation in Obese Adults in Peripheral Blood Cells and MSH Neurons

Initially, we performed bisulfite pyrosequencing at each of nine *POMC*-VMR-CpG-sites to reproduce our previous finding of hypermethylation in obese compared to normal-weight children (Kuehnen et al., 2012). As in the previous study, we found a significant positive correlation of methylation across CpG sites −2 to +5 with individual BMI SD score (SDS) (Figure S1). Thereafter, we analyzed this region in obese versus normal-weight adult individuals. We again found variable methylation at the border of intron 2/exon 3 and significant hypermethylation at positions +1, +2, +3, and +5 (Figure 1B). Moreover, we found a significant positive correlation of average methylation across CpG sites −2 to +5 with BMI ($r = 0.18$, $p = 0.006$) (Figure 1C).

We next performed laser microdissection of MSH-positive arcuate nucleus neurons from postmortem human brain. *POMC* gene expression in those neurons is most crucial for individual body-weight regulation. Laser-microdissected MSH-positive neurons were collected from 41 obese and normal-weight individuals (Figure S1), and the methylation status was analyzed by bisulfite pyrosequencing (see Experimental Procedures). Again, we observed variable methylation at the intron 2/exon 3 border, and *POMC* methylation across sites −2 to +5 of the MSH neurons was positively correlated with individual BMI ($r = 0.34$, $p = 0.025$) (Figure 1D). Together with our previous finding that hypermethylation at positions −2 to +5 decreases *POMC* gene expression (Kuehnen et al., 2012), it is likely that hypermethylation of the *POMC* gene in MSH neurons from obese individuals results in a lower expression of *POMC* gene product, which might inhibit normal satiety responses and promote obesity. This correlation would imply that a 10% increase in methylation is associated with 2.8 kg/m^2 increase in BMI ($p = 0.025$) (Figure 1D), a much stronger effect than observed for top genome-wide association study (GWAS) SNPs associated with obesity, such as at *FTO* (0.39 kg/m^2 per allele) (Loos, 2012; Murphy and Mill, 2014).

Non-tissue Specificity of POMC Methylation

We analyzed the extent of systemic (cross-tissue) variation in *POMC* methylation. A comparison of *POMC* methylation of neurons within the arcuate nucleus with methylation in PBCs in a subset of 14 postmortem-studied individuals revealed a strong positive correlation ($r = 0.63$, $p = 0.014$) (Figure 2A), suggesting that cells from different germ layers—ectoderm (brain) and mesoderm (PBCs)—maintain a similar methylation level. We further confirmed this by analyzing an independent second set of tissue samples from different individuals (see Experimental Procedures). Again, we found high intra-individual correlation of methylation in ectoderm (brain) and mesoderm (kidney) samples ($r = 0.7$, $p = 0.002$) (Figure 2B). These data argue that methylation across the *POMC* VMR may be established very early during development, before separation of germ layers at gastrulation.

Longitudinal Stability of POMC Methylation

To further test the longitudinal stability of interindividual variation in *POMC* methylation, we analyzed the methylation in DNA extracted from newborn screening cards (a blood collection that is routinely performed after birth between day 3 and 10 postpartum) and compared this with the *POMC* methylation status of the same individual in a second blood collection performed later in life ($n = 52$; mean time span, 11.69 years; range, 3–24 years). We observed a strong correlation of methylation within individuals across this time period (Figure 2C), indicating that the *POMC* methylation pattern is stable over time and not strongly influenced by postnatal environment.

Impact of Genetic Variation in *cis* on POMC Methylation

Several epigenome-wide association studies (EWASs) have identified methylation variants (meQTL) associated with SNPs

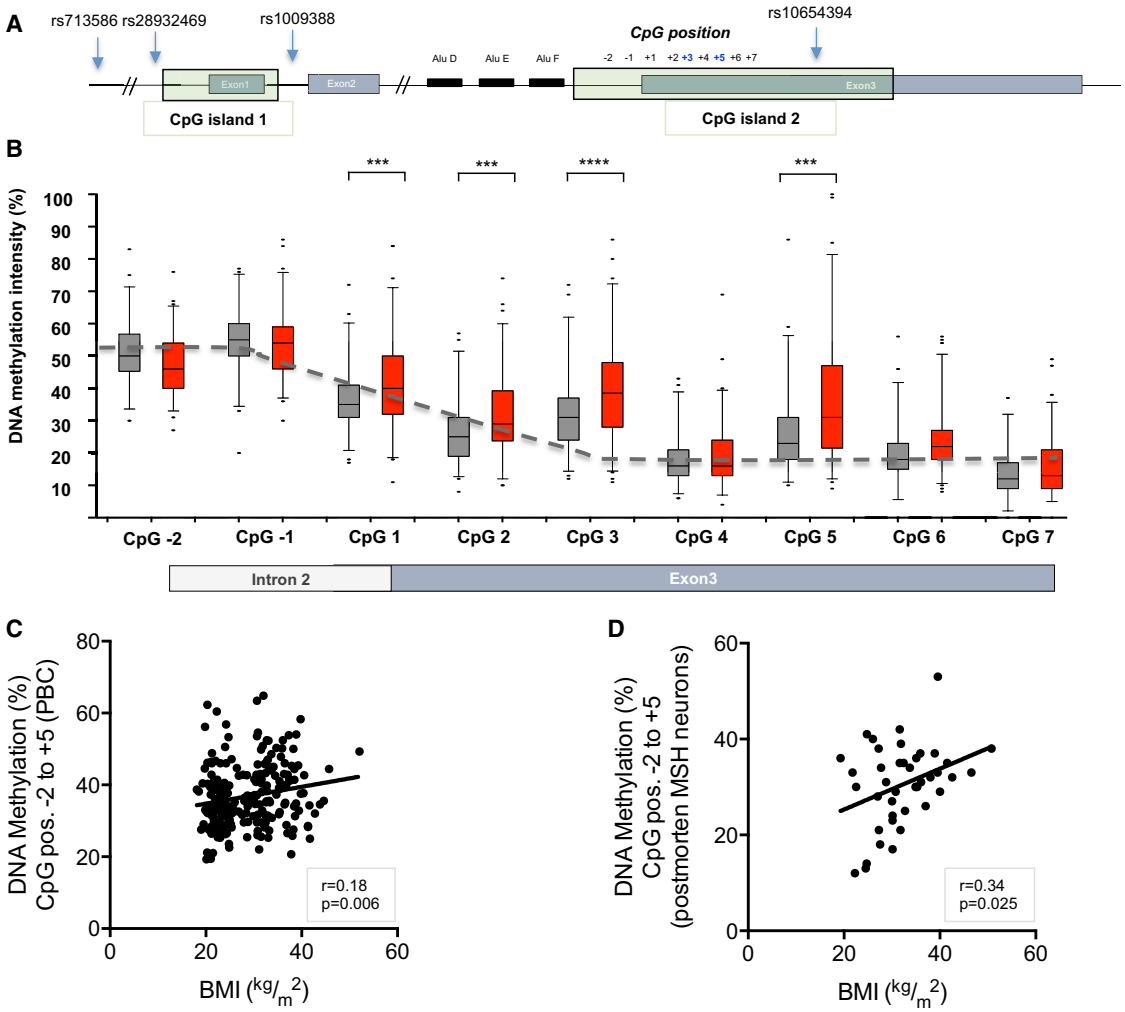

Figure 1. *POMC* Gene Structure and Pyrosequencing Results in an Adult Cohort

(A) The *POMC* gene structure indicating the location of CpG islands (green), the Alu elements (black boxes) and CpGs −2 to +7, which were analyzed by pyrosequencing.

(B) Bisulfite-pyrosequencing analysis of DNA methylation in peripheral blood cells from 103 normal-weight (gray) and 125 obese (red) adult individuals. The most significant differences were observed at CpG positions +3 and +5 (corresponding to nucleotide number chr2:25.384.590 and chr2:25.384.569 [UCSC human genome browser hg19]). The gray dotted line shows the variation in mean methylation values from the intron (CpG positions −2 and −1) to the exon at CpG positions +4 to +7. Error bars represent SD.

(C and D) Linear regression based on the mean value of CpG positions −2 to +5 and BMI in the German adult cohort (n = 228) (C) and MSH laser-microdissected neurons from postmortem human brain samples (n = 41) (D).

in *cis* (Dick et al., 2014), implying that they may simply represent secondary epigenetic differences resulting from genetic variation (Murphy and Mill, 2014). We searched for meQTL at *POMC* by sequencing the entire region of the *POMC* gene, including the promoter and 3′ UTR, in two cohorts of normal-weight children of different genetic (European and West African) origin (see Experimental Procedures). None of the genetic variants present, including rs713586 (the only known BMI-associated *POMC* SNP identified in a GWAS meta-analysis; Speliotes et al., 2010), was associated with methylation across the nine VMR-CpGs (Figures S2A and S2B). In addition, although the African and European cohorts show significant differences in their SNP characteristics (Figures S2A and S2B), average *POMC* methylation in both cohorts was essentially identical (Figure S2C). It is therefore unlikely that the *POMC* methylation variant is driven by a genetic polymorphism.

Paternal Impact on POMC Methylation

To further analyze a potential genetic effect on the *POMC* methylation variant, we investigated the inheritance of methylation status at the *POMC* VMR in 47 family trios of obese children and their parents. Notably, methylation of a child's *POMC* VMR correlated only with its father's *POMC* methylation level (Figure 3A) and not with that of its mother (Figure 3B). These data suggest a partial transmission of the *POMC* VMR methylation state through the paternal germline that is not driven by genetic variation. To investigate the underlying mechanism explaining this correlation between paternal and offspring methylation, we

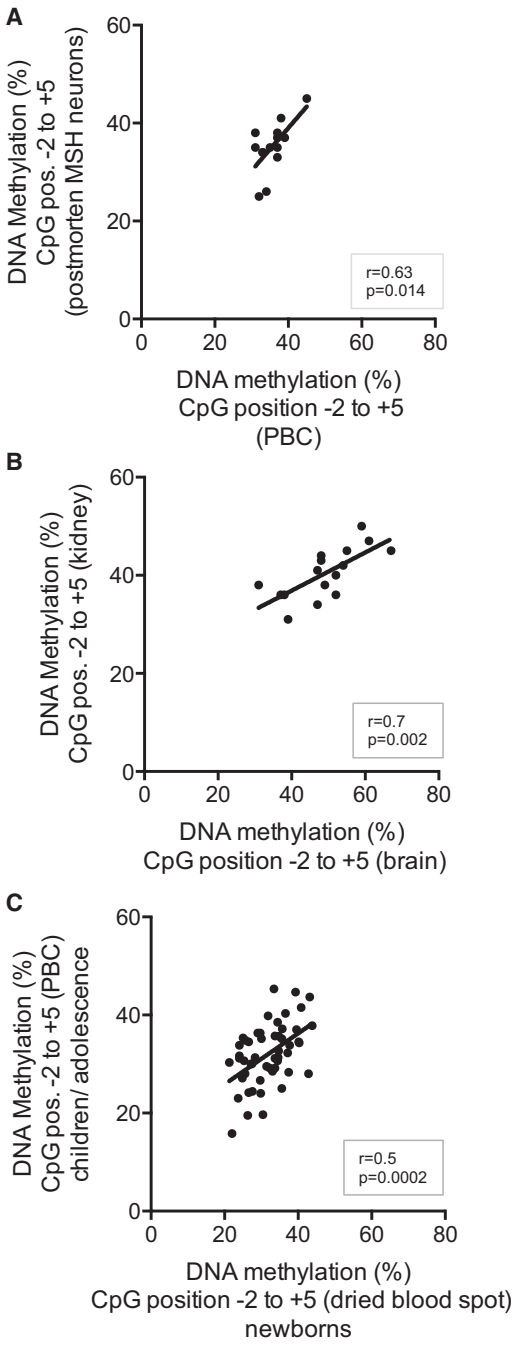

Figure 2. Cross-Tissue Correlations in Intra-individual *POMC* Methylation and Stability over Time

(A) *POMC* DNA methylation at CpG positions −2 to +5 correlates significantly between laser-microdissected MSH neurons and laser-microdissected blood cells (n = 14).

(B) Intra-individual correlation between the *POMC* DNA methylation (%) at CpG positions −2 to +5 of postmortem human brain and kidney tissues.

(C) Longitudinal stability of DNA methylation in the same individuals measured perinatally and in adolescence (n = 52).

analyzed *POMC* methylation in sperm and blood (PBC) DNA of 17 German men. Interestingly, *POMC* VMR methylation was significantly lower in sperm than in blood (Figure S3A), consistent with a loss of methylation during germline differentiation as has been shown for imprinted regions (Monk, 2015). However, PBC methylation is correlated with BMI in the same individuals ($r = 0.54$, $p = 0.025$) (Figure S3B). These data suggest that paternal transmission of the epigenetic state at the *POMC* VMR occurs by some mechanism other than DNA methylation.

POMC Methylation Is Not Influenced by Maternal Body-Weight Changes during Pregnancy

To further search for the origin of *POMC* VMR methylation we assessed the potential influence of the early in utero environment. We analyzed 33 European mother-child pairs and tested for a correlation of maternal body weight during pregnancy with the child's *POMC* methylation level. Neither maternal body weight at conception nor weight change during pregnancy was correlated with the *POMC* methylation level determined in the child's PBC DNA (Figure S3).

POMC Methylation Is Influenced by One-Carbon Metabolism

Establishment of DNA methylation at human MEs has shown to be sensitive to C1 metabolites at the time of conception. C1 metabolism is central because it regulates the supply of methyl groups required for DNA methylation. Betaine and 5-methyltetrahydrofolate are methyl donors for the methylation of methionine, converting it to S-adenosylmethionine (SAM). In transmethylation reactions, SAM donates a methyl group and is transformed into S-adenosylhomocysteine (SAH), which is then metabolized into homocysteine. To analyze the impact of these C1 metabolites on *POMC* methylation, we investigated a West African cohort of 144 mother-child pairs from a rural area of The Gambia, in which data on maternal periconceptional C1 metabolites were available (Dominguez-Salas et al., 2014). In this region, the alternation of rainy and dry seasons leads to large changes in the environment affecting maternal nutrition and the supply of C1-metabolites (Dominguez-Salas et al., 2013). We found lower DNA methylation at the *POMC* VMR in children conceived in the dry season compared to those conceived in the rainy season (Table 1), consistent with previous observations at known MEs (Dominguez-Salas et al., 2014; Silver et al., 2015). Testing for a direct influence of maternal serum C1-metabolites, a robust and significant negative correlation for SAH and positive correlations with betaine and the ratio of SAM to SAH were found at all CpGs from −2 to +7 (Tables 1 and 2; Experimental Procedures).

DISCUSSION

Our findings in different obese cohorts and postmortem studies indicate that methylation of the human *POMC* VMR is correlated with individual body weight. The finding of reduced *POMC* gene expression in the presence of the hypermethylated variant (Kuehnen et al., 2012), together with our observation that the same association is observed in MSH-positive arcuate nucleus neurons, suggests that hypermethylation at the *POMC* VMR may be functionally related to an individual's body weight.

In addition, the findings in the present study imply that the *POMC* VMR shares a set of common characteristics with the

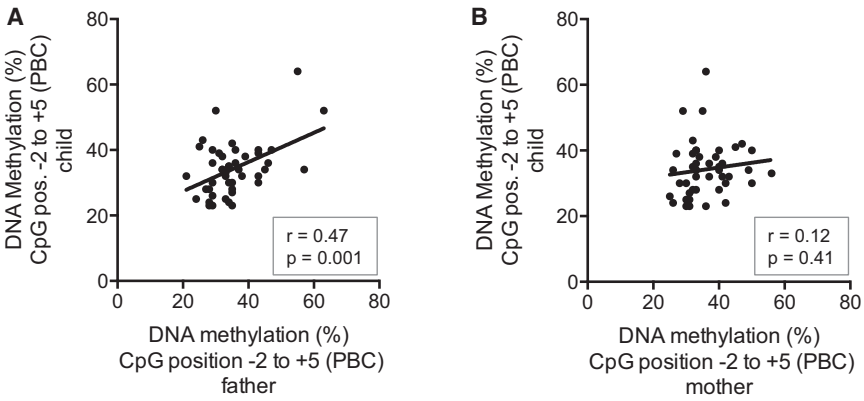

Figure 3. *POMC* Pyrosequencing Analysis in Family Trios with One Obese Child

Peripheral blood DNA samples from 47 trio families, each with one obese child, were analyzed by pyrosequencing.

(A) Correlation between paternal and offspring DNA methylation at CpG positions −2 to +5.

(B) Correlation between maternal and offspring DNA methylation CpG positions −2 to +5.

mouse A^{vy} locus. Namely, it is (1) triggered by a transposable element, (2) sensitive to nutritional modification by C1 metabolites during early embryonic development, (3) in part transmitted via one parental germline, (4) stable over the life course, and (5) correlated with body weight. In addition, our data argue against an influence of maternal body weight during pregnancy and of genetic variation at the *POMC* gene locus. In this respect, the observed *POMC* VMR methylation differs fundamentally from other identified methylation variants that are associated with obesity, which result either from non-inherited environmental influences or represent secondary epigenetic differences resulting primarily from genetic variation (Murphy and Mill, 2014).

Together, these complementary data across multiple populations argue that the variation of the *POMC* VMR resembles a metastable epiallele, like those described in the mouse A^{vy} locus. As already shown for the A^{vy} locus, methylation of the *POMC* VMR appears to be established before the separation of the germ layers during the very early stages of genome re-methylation, resulting in significant correlation of methylation levels across somatic cell types derived from different germ layers. We cannot, however, exclude the possibility that an environmental exposure in adulthood may influence methylation patterns in multiple tissues. Additionally, early embryonic establishment of *POMC* VMR methylation appears to be influenced by the availability of C1 metabolites in the maternal circulation around the time of conception. Our data also point to the influence of some other factor transmitted from the father to the offspring, although the mechanism is unknown. One possibility is the transmission of sperm microRNAs (Gapp et al., 2014; Wagner et al., 2008). Our interpretation of these various observations is that *POMC* methylation is determined combinatorially by stochastic epigenetic events during early embryonic development (which are influenced by maternal nutrition) and by non-genetic paternal transmission, although further studies in independent samples will be required to confirm that the *POMC* VMR is acting as a metastable epiallele.

Importantly, our data indicating early embryonic establishment and long-term stability of methylation at the *POMC* VMR help inform causality. In particular, together with our findings showing that methylation at this locus is correlated with individual BMI, these data suggest that individual epigenetic variation at the *POMC* VMR is a cause rather than a consequence of obesity. Moreover, if stochastic establishment of DNA methylation at the *POMC* VMR occurs before the embryo cleavage that results in monozygotic (MZ) twins, this could lead to a shared *POMC* VMR epigenotype in monozygotic twins, independent of their genetic identity (Waterland et al., 2010). This may offer a partial explanation for the missing heritability of BMI (Llewellyn et al., 2013).

EXPERIMENTAL PROCEDURES

All procedures and measurements were approved by the Ethics Committee of the Charité Universitätsmedizin Berlin (EA2/131/11, EA1/019/13 and EA2/116/10), the Universitätsklinikum Essen (05-2954), the joint Gambian Government/MRC Unit, and the Gambia Ethics Committee (L2013.25) and according to the declaration of Helsinki. The patients and/or their parents/guardians gave informed consent.

POMC Genotyping Analysis

The genomic *POMC* region was analyzed in DNA samples from a European cohort (Berlin, Charité Universitätsmedizin Berlin) and from the Gambian cohort (infants) by traditional Sanger sequencing on an ABI Sequencer (Applied Biosystems 3130xl, Genetic Analyzer). For oligo sequences and further details, please see Supplemental Information (Table S1).

DNA Methylation Analysis

DNA (500 ng) for German cohorts was extracted according to standard protocols (Promega) from PBCs. For Gambians, DNA was extracted from venous blood using a standard salting-out method (Miller et al., 1988). The samples were converted with sodium-bisulfite (EpiTect-Kit, QIAGEN). For further details of methylation analysis and DNA extraction, see Supplemental Experimental Procedures.

Study Cohorts

Adult Case-Control Cohort

The control group consists of 103 normal-weight adults with a mean age of 48.2 ± 11.74 years and a mean BMI of 22.5 ± 1.65 kg/m^2 (32 males, 71 females). The obese group includes 125 individuals with a mean age of 54.2 ± 8.35 years and a mean BMI of 36.03 ± 5.61 kg/m^2 (50 males, 75 females). The samples were part of the MesyBepo follow-up study (Bobbert et al., 2013).

Family Trios

A total of 47 family trios each with one obese child (mean age 13.23 ± 2.34 years, mean BMI 30.2 ± 4.34 kg/m^2) were analyzed. The fathers had a mean age of 44.53 ± 8.06 years and a mean BMI of 28.6 ± 5.73 kg/m^2. The mothers had a mean age of 41.11 ± 4.11 years and a mean BMI of 28.37 ± 8.33 kg/m^2.

European Healthy Children Analyzed for Genetic Variant

Eighty-four normal-weight children with a mean BMI of 18 ± 0.61 kg/m^2 and a mean age of 8.9 ± 2.01 years (44 females, 40 males), recruited in the outpatient clinic of the Department of Pediatric Endocrinology, Charité Universitätsmedizin Berlin, were analyzed.

Table 1. Correlations between Maternal Biomarker Status around Conception and Offspring DNA Methylation

Covariate	Coef	SE	z value	p value	[95% CI]	
Season (dry)	−0.152	0.07	−2.14	0.034	−0.291	−0.012
Folate	0.070	0.09	0.79	0.432	−0.106	0.247
B12	0.017	0.09	0.18	0.854	−0.164	0.197
B2	−0.108	0.15	−0.73	0.467	−0.402	0.185
B6	−0.071	0.10	−0.71	0.482	−0.270	0.128
Choline	0.095	0.12	0.78	0.437	−0.146	0.336
Betaine	0.275	0.10	2.80	0.006	0.081	0.470
Methionine	0.211	0.19	1.13	0.262	−0.160	0.583
Cysteine	0.158	0.30	0.53	0.594	−0.429	0.746
Homocysteine	−0.187	0.11	−1.67	0.098	−0.410	0.035
DMG	0.002	0.06	0.03	0.975	−0.125	0.129
SAM	−0.135	0.22	−0.62	0.537	−0.568	0.297
SAH	−0.353	0.10	−3.57	0.001	−0.549	−0.157
SAM:SAH ratio	0.340	0.10	3.34	0.001	0.138	0.541
Betaine:DMG ratio	0.093	0.06	1.59	0.114	−0.022	0.208
BMI	−0.006	0.01	−0.53	0.599	−0.029	0.017

Environmental impact on peripheral blood DNA methylation in 144 children from The Gambia who were conceived during either the dry season or the rainy season. DNA methylation was analyzed against maternal periconceptional methyl-donor biomarker status (Dominguez-Salas et al., 2014). Season of conception, maternal betaine, SAH, and the SAM:SAH ratio predict offspring mean methylation across the *POMC* VMR. CI, confidence interval; Coef, coefficient; CpG, CpG site within *POMC* locus; DMG, dimethylglycine; p, p value; SAM, s-adenosylmethionine; SAH, s-adenosylhomocysteine; z, z value.

Table 2. Correlation between Each Analyzed CpG Position and the Maternal Serum Concentration of SAH, SAM:SAH, and Betaine during Conception

Predictor	CpG	Coef	SE	z	p	[95% CI]	
SAH	−2	−0.29	0.10	−2.99	0.003	−0.47	−0.10
	−1	−0.33	0.11	−2.95	0.004	−0.55	−0.11
	1	−0.41	0.11	−3.58	< 0.001	−0.63	−0.18
	2	−0.32	0.14	−2.30	0.023	−0.60	−0.05
	3	−0.34	0.12	−2.76	0.007	−0.59	−0.10
	4	−0.32	0.12	−2.63	0.009	−0.57	−0.08
	5	−0.59	0.16	−3.58	< 0.001	−0.91	−0.26
	6	−0.40	0.12	−3.34	0.001	−0.64	−0.16
	7	−0.32	0.16	−2.00	0.048	−0.64	0.01
SAM:SAH	−2	0.21	0.10	2.11	0.036	0.01	0.40
	−1	0.23	0.11	2.08	0.039	0.01	0.46
	1	0.33	0.12	2.81	0.006	0.10	0.56
	2	0.24	0.14	1.66	0.099	−0.05	0.52
	3	0.28	0.13	2.23	0.028	0.03	0.53
	4	0.23	0.12	1.83	0.070	−0.02	0.47
	5	0.58	0.17	3.50	0.001	0.25	0.91
	6	0.35	0.12	2.92	0.004	0.11	0.59
	7	0.25	0.16	1.58	0.117	−0.06	0.57
Betaine	−2	0.04	0.09	0.46	0.647	−0.14	0.23
	−1	0.07	0.11	0.64	0.525	−0.14	0.28
	1	0.10	0.11	0.89	0.378	−0.12	0.32
	2	0.34	0.13	2.63	0.010	0.08	0.59
	3	0.32	0.12	2.69	0.008	0.08	0.56
	4	0.35	0.11	3.03	0.003	0.12	0.57
	5	0.28	0.16	1.72	0.088	−0.04	0.60
	6	0.37	0.11	3.23	0.002	0.14	0.60
	7	0.16	0.15	1.09	0.278	−0.13	0.46

Summary of SAM, SAM:SAH ratio, and betaine-dependent DNA methylation at individual *POMC* CpG positions −2 to +7. Associations between SAH, SAM:SAH, and methylation show no significant differential effect with CpG site. Methylation associated with betaine varies by CpG site (see Gambian Cohort Analyses Section in Supplemental Information). CI, confidence interval; Coef, coefficient; CpG, CpG site within *POMC* locus; p, p value; SAM, s-adenosylmethionine; SAH, s-adenosylhomocysteine; z, z value.

European Normal-Weight and Obese Children and Mother-Child Pairs Analyzed for POMC Methylation

Seventy-six normal-weight patients (37 females, 39 males; average age, 5.7 ± 5.5 years; average BMI, 17.3 ± 3 kg/m^2) and 83 obese patients (43 females, 40 males; average age, 13.7 ± 1.9 years; average BMI, 30.83 ± 4.2 kg/m^2) were recruited in the outpatient clinic of the Department of Pediatric Endocrinology of the Charité Universitätsmedizin Berlin. From 33 obese patients (20 females, 13 males; average age, 13.4 years; average BMI, 30.6 kg/m^2), data on the body-weight course of the mother during pregnancy were available. None of the mothers had gestational diabetes.

Gambian Mother-Infant Pairs

Samples originate from an observational prospective study (registered at https://www.clinicaltrials.gov, reference NCT01811641) in The Gambia, West Africa, assessing season of conception and maternal nutritional status on infant epigenetic outcomes (Dominguez-Salas et al., 2013, 2014). For details, see Supplemental Experimental Procedures.

Human Tissue Samples

Postmortem samples of 16 Vietnamese motor vehicle accident victims (Waterland et al., 2010) were collected at the human tissue bank (ILSbio).

Longitudinal Analysis of DNA Methylation

The *POMC* DNA methylation pattern has been analyzed longitudinally from the same individual (n = 51 [24 females, 27 males]; BMI, 27.92 ± 6.8 kg/m^2). The first sample was extracted from the newborn screening card (routinely performed blood collection between days 3 and 10 in Germany). The second sample originated from a blood collection at an age of 11.69 ± 5.5 years.

Postmortem Human Brain Tissue Samples

Hypothalamic samples of 41 individuals were obtained from autopsies performed according to Berlin law (Sektionsgesetz, Gesetz- und Verordnungsblatt für Berlin, 1996; 52 32, 237–239) from the Department of Neuropathology, Charité Universitätsmedizin Berlin. Subjects were selected with no history of neurodegenerative diseases or cancer (12 females, 29 males; average age, 67 ± 12.76 years; average BMI, 32.3 ± 6.8 kg/m^2). For technical details, especially on laser microdissection and immunostaining, see Supplemental Experimental Procedures.

Sperm-PBC Sample Pairs

Sperm and PBC DNA pairs from the same male obese (n = 7; mean age, 36.4 years; BMI, 31.9 kg/m^2) and non-obese (n = 10; mean age, 36.5 years; BMI, 23.01 kg/m^2) individual were obtained from the Center of Reproductive Medicine and Andrology, Münster, Germany (Prof. Gromoll). DNA was extracted as described previously (Laurentino et al., 2015).

Statistical Analysis

The DNA methylation at CpG positions −2 to +7 (nine CpG positions in total, CpG positions −2 to +5, or each CpG position separately) was statistically analyzed by Student's t test. All results were adjusted for age and sex. The linear regression between BMI and DNA methylation at position −2 to +5 was tested as an exploratory analysis. The DNA methylation mean value of

CpG positions −2 to +5 was analyzed against the BMI after Bonferroni correction for multiple testing (p = 0.0005). The logistic regression was calculated with a BMI above 30 kg/m^2 as a binary outcome to obtain the risk for becoming obese. The calculations were performed with PASW (SPSS 21). For further details, especially on the Gambian C1 analysis, see Supplemental Experimental Procedures. Error bars represent SD.

SUPPLEMENTAL INFORMATION

Supplemental Information includes Supplemental Experimental Procedures, three figures, and two tables and can be found with this article online at http://dx.doi.org/10.1016/j.cmet.2016.08.001.

AUTHOR CONTRIBUTIONS

P.K. and H.K. designed the study. P.K. and D.H. performed functional experiments. L.W. performed the analysis of DNA extracted from newborn screening cards. A.H. and J.H. provided samples from family trios. B.J.H., A.M.P., M.S., P.D.-S., and S.E.M. provided samples and information for the Gambian mother-infant cohort. R.A.W. provided the samples from human postmortem kidney and brain tissue. A.G. was involved in results-discussion. J.S. provided samples from normal-weight and obese adults. A.J.F. performed the statistical analysis of the Gambian cohort. F.L.H. provided postmortem brain tissue for laser microdissection. C.G. provided the facility for laser microdissection. J.G. provided sperm and blood DNA sample pairs. S.W. provided the samples from the outpatient clinic of the Institute for Experimental Pediatric Endocrinology, Charité, Universitätsmedizin Berlin. P.K., H.K., B.J.H, A.P., M.S., and R.A.W. wrote the manuscript with the contributions of all other co-authors.

ACKNOWLEDGMENTS

This work was supported by grants from the German Research Foundation (DFG) (KU 2673/2-1, KFO218, GK-1208, and HI 865/2-1), BMBF (NGFN-Plus, 01GS0820), and the Helmholz Association (ICEMED). P.K. was supported by the Charité/Berlin Institute of Health (BIH) Clinical Scientist Program. H.K. was supported by the Berlin Institute of Health (BIH). R.A.W. was supported by grants from NIH/National Institute of Diabetes and Digestive and Kidney Diseases (1R01DK081557) and the USDA (CRIS 6250-51000-055). C.G. was supported by grants 03IP614 and 03IPT614A from the German Ministry for Education and Research (BMBF). The Gambian study was supported by a Wellcome Trust grant WT086369MA (to B.J.H.) and core funding MC-A760-5QX00 to the MRC International Nutrition Group by the UK Medical Research Council (MRC) and the UK Department for the International Development (DFID) under the MRC/DFID Concordat agreement. Our thanks go to the study participants from The Gambia and staff at MRC Keneba, The Gambia and Rita Oeltjen for excellent technical assistance.

Received: December 22, 2015
Revised: May 17, 2016
Accepted: July 28, 2016
Published: August 25, 2016

REFERENCES

Bobbert, T., Schwarz, F., Fischer-Rosinsky, A., Pfeiffer, A.F., Möhlig, M., Mai, K., and Spranger, J. (2013). Fibroblast growth factor 21 predicts the metabolic syndrome and type 2 diabetes in Caucasians. Diabetes Care *36*, 145–149.

Dalgaard, K., Landgraf, K., Heyne, S., Lempradl, A., Longinotto, J., Gossens, K., Ruf, M., Orthofer, M., Strogantsev, R., Selvaraj, M., et al. (2016). Trim28 Haploinsufficiency Triggers Bi-stable Epigenetic Obesity. Cell *164*, 353–364.

Dick, K.J., Nelson, C.P., Tsaprouni, L., Sandling, J.K., Aïssi, D., Wahl, S., Meduri, E., Morange, P.E., Gagnon, F., Grallert, H., et al. (2014). DNA methylation and body-mass index: a genome-wide analysis. Lancet *383*, 1990–1998.

Dominguez-Salas, P., Moore, S.E., Cole, D., da Costa, K.A., Cox, S.E., Dyer, R.A., Fulford, A.J., Innis, S.M., Waterland, R.A., Zeisel, S.H., et al. (2013). DNA methylation potential: dietary intake and blood concentrations of one-carbon metabolites and cofactors in rural African women. Am. J. Clin. Nutr. *97*, 1217–1227.

Dominguez-Salas, P., Moore, S.E., Baker, M.S., Bergen, A.W., Cox, S.E., Dyer, R.A., Fulford, A.J., Guan, Y., Laritsky, E., Silver, M.J., et al. (2014). Maternal nutrition at conception modulates DNA methylation of human metastable epialleles. Nat. Commun. *5*, 3746.

Eichler, E.E., Flint, J., Gibson, G., Kong, A., Leal, S.M., Moore, J.H., and Nadeau, J.H. (2010). Missing heritability and strategies for finding the underlying causes of complex disease. Nat. Rev. Genet. *11*, 446–450.

Elks, C.E., den Hoed, M., Zhao, J.H., Sharp, S.J., Wareham, N.J., Loos, R.J., and Ong, K.K. (2012). Variability in the heritability of body mass index: a systematic review and meta-regression. Front Endocrinol. (Lausanne) *3*, 29.

Farooqi, I.S., Drop, S., Clements, A., Keogh, J.M., Biernacka, J., Lowenbein, S., Challis, B.G., and O'Rahilly, S. (2006). Heterozygosity for a POMC-null mutation and increased obesity risk in humans. Diabetes *55*, 2549–2553.

Gapp, K., Jawaid, A., Sarkies, P., Bohacek, J., Pelczar, P., Prados, J., Farinelli, L., Miska, E., and Mansuy, I.M. (2014). Implication of sperm RNAs in transgenerational inheritance of the effects of early trauma in mice. Nat. Neurosci. *17*, 667–669.

Koza, R.A., Nikonova, L., Hogan, J., Rim, J.S., Mendoza, T., Faulk, C., Skaf, J., and Kozak, L.P. (2006). Changes in gene expression foreshadow diet-induced obesity in genetically identical mice. PLoS Genet. *2*, e81.

Krude, H., Biebermann, H., Luck, W., Horn, R., Brabant, G., and Grüters, A. (1998). Severe early-onset obesity, adrenal insufficiency and red hair pigmentation caused by POMC mutations in humans. Nat. Genet. *19*, 155–157.

Krude, H., Biebermann, H., Schnabel, D., Tansek, M.Z., Theunissen, P., Mullis, P.E., and Grüters, A. (2003). Obesity due to proopiomelanocortin deficiency: three new cases and treatment trials with thyroid hormone and ACTH4-10. J. Clin. Endocrinol. Metab. *88*, 4633–4640.

Kuehnen, P., Mischke, M., Wiegand, S., Sers, C., Horsthemke, B., Lau, S., Keil, T., Lee, Y.A., Grueters, A., and Krude, H. (2012). An Alu element-associated hypermethylation variant of the POMC gene is associated with childhood obesity. PLoS Genet. *8*, e1002543.

Laurentino, S., Beygo, J., Nordhoff, V., Kliesch, S., Wistuba, J., Borgmann, J., Buiting, K., Horsthemke, B., and Gromoll, J. (2015). Epigenetic germline mosaicism in infertile men. Hum. Mol. Genet. *24*, 1295–1304.

Llewellyn, C.H., Trzaskowski, M., Plomin, R., and Wardle, J. (2013). Finding the missing heritability in pediatric obesity: the contribution of genome-wide complex trait analysis. Int. J. Obes. *37*, 1506–1509.

Locke, A.E., Kahali, B., Berndt, S.I., Justice, A.E., Pers, T.H., Day, F.R., Powell, C., Vedantam, S., Buchkovich, M.L., Yang, J., et al.; LifeLines Cohort Study; ADIPOGen Consortium; AGEN-BMI Working Group; CARDIOGRAMplusC4D Consortium; CKDGen Consortium; GLGC; ICBP; MAGIC Investigators; MuTHER Consortium; MIGen Consortium; PAGE Consortium; ReproGen Consortium; GENIE Consortium; International Endogene Consortium (2015). Genetic studies of body mass index yield new insights for obesity biology. Nature *518*, 197–206.

Loos, R.J. (2012). Genetic determinants of common obesity and their value in prediction. Best Pract. Res. Clin. Endocrinol. Metab. *26*, 211–226.

Miller, S.A., Dykes, D.D., and Polesky, H.F. (1988). A simple salting out procedure for extracting DNA from human nucleated cells. Nucleic Acids Res. *16*, 1215.

Monk, D. (2015). Germline-derived DNA methylation and early embryo epigenetic reprogramming: The selected survival of imprints. Int. J. Biochem. Cell Biol. *67*, 128–138.

Morgan, H.D., Sutherland, H.G., Martin, D.I., and Whitelaw, E. (1999). Epigenetic inheritance at the agouti locus in the mouse. Nat. Genet. *23*, 314–318.

Murphy, T.M., and Mill, J. (2014). Epigenetics in health and disease: heralding the EWAS era. Lancet *383*, 1952–1954.

Radford, E.J., Ito, M., Shi, H., Corish, J.A., Yamazawa, K., Isganaitis, E., Seisenberger, S., Hore, T.A., Reik, W., Erkek, S., et al. (2014). In utero effects. In utero undernourishment perturbs the adult sperm methylome and intergenerational metabolism. Science *345*, 1255903.

Rakyan, V.K., Blewitt, M.E., Druker, R., Preis, J.I., and Whitelaw, E. (2002). Metastable epialleles in mammals. Trends Genet. *18*, 348–351.

Rakyan, V.K., Chong, S., Champ, M.E., Cuthbert, P.C., Morgan, H.D., Luu, K.V., and Whitelaw, E. (2003). Transgenerational inheritance of epigenetic states at the murine Axin(Fu) allele occurs after maternal and paternal transmission. Proc. Natl. Acad. Sci. USA *100*, 2538–2543.

Silver, M.J., Kessler, N.J., Hennig, B.J., Dominguez-Salas, P., Laritsky, E., Baker, M.S., Coarfa, C., Hernandez-Vargas, H., Castelino, J.M., Routledge, M.N., et al. (2015). Independent genomewide screens identify the tumor suppressor VTRNA2-1 as a human epiallele responsive to periconceptional environment. Genome Biol. *16*, 118.

Speliotes, E.K., Willer, C.J., Berndt, S.I., Monda, K.L., Thorleifsson, G., Jackson, A.U., Lango Allen, H., Lindgren, C.M., Luan, J., Mägi, R., et al.; MAGIC; Procardis Consortium (2010). Association analyses of 249,796 individuals reveal 18 new loci associated with body mass index. Nat. Genet. *42*, 937–948.

Tamashiro, K.L., Wakayama, T., Akutsu, H., Yamazaki, Y., Lachey, J.L., Wortman, M.D., Seeley, R.J., D'Alessio, D.A., Woods, S.C., Yanagimachi, R., and Sakai, R.R. (2002). Cloned mice have an obese phenotype not transmitted to their offspring. Nat. Med. *8*, 262–267.

Wagner, K.D., Wagner, N., Ghanbarian, H., Grandjean, V., Gounon, P., Cuzin, F., and Rassoulzadegan, M. (2008). RNA induction and inheritance of epigenetic cardiac hypertrophy in the mouse. Dev. Cell *14*, 962–969.

Waterland, R.A. (2014). Epigenetic mechanisms affecting regulation of energy balance: many questions, few answers. Annu. Rev. Nutr. *34*, 337–355.

Waterland, R.A., and Jirtle, R.L. (2003). Transposable elements: targets for early nutritional effects on epigenetic gene regulation. Mol. Cell. Biol. *23*, 5293–5300.

Waterland, R.A., Dolinoy, D.C., Lin, J.R., Smith, C.A., Shi, X., and Tahiliani, K.G. (2006). Maternal methyl supplements increase offspring DNA methylation at Axin Fused. Genesis *44*, 401–406.

Waterland, R.A., Kellermayer, R., Laritsky, E., Rayco-Solon, P., Harris, R.A., Travisano, M., Zhang, W., Torskaya, M.S., Zhang, J., Shen, L., et al. (2010). Season of conception in rural gambia affects DNA methylation at putative human metastable epialleles. PLoS Genet. *6*, e1001252.

Yang, J., Bakshi, A., Zhu, Z., Hemani, G., Vinkhuyzen, A.A., Lee, S.H., Robinson, M.R., Perry, J.R., Nolte, I.M., van Vliet-Ostaptchouk, J.V., et al.; LifeLines Cohort Study (2015). Genetic variance estimation with imputed variants finds negligible missing heritability for human height and body mass index. Nat. Genet. *47*, 1114–1120.